Probing anomalous Wtb couplings at the LHC in single t-channel top quark production

Adil Jueid*

INPAC, Shanghai Key Laboratory for Particle Physics and Cosmology, Department of Physics and Astronomy, Shanghai Jiao Tong University, Shanghai 200240, China and Département de Mathématiques, Faculté des Sciences et Techniques, Université Abdelmalek Essaadi, B. 416 Tangier, Morocco

(Received 12 June 2018; published 25 September 2018)

We study the sensitivity of certain observables to the anomalous right tensorial coupling in single top production at the LHC at $\sqrt{s} = 13$ TeV. The observables consist of asymmetries constructed from the energy and angles of the decay products of the top quark produced in single top production through the t-channel. The computation is done at leading order (LO) and next-to-leading order (NLO) in the strong coupling in the five-flavor scheme. We have estimated projected limits on the anomalous coupling, both at the parton level without cuts and at the particle level with cuts. We find that the asymmetries are robust with respect to the higher-order QCD corrections and are indeed a very good probe of this anomalous coupling of the top. Hence, they can be used as experimental probes of the same.

DOI: 10.1103/PhysRevD.98.053006

I. INTRODUCTION

Top quark is the heaviest among all the SM particles. This particle was discovered at the Tevatron-Fermilab by CDF [1] and D0 [2] collaborations. It has a pole mass $m_t = 173.1 \pm 0.6$ GeV [3] which is very close to the electroweak symmetry breaking scale. Due to its large mass, it can only be created at high energy experiments such as the Tevatron or the LHC with a reasonable number. The top quark plays an important role in high energy physics as it is believed that, due its large mass, effects of new physics beyond the SM can be easily shown [4–6]. Top quark is dominantly produced at the LHC, through QCD, in the pair mode with a cross section approaching one nanobarn at $\sqrt{s} = 13$ TeV. Due to the vector nature of the strong interaction, the produced top quark pairs are unpolarised. In addition to the pair production mode, top quark can be produced in association with a lighter particle. This production mechanism proceeds through electroweak interaction. Hence, it has a smaller cross section, the maximum being ∼140 pb. However, the $V - A$ nature of the charged current interaction implies that the top quark produced in association are polarized. The much smaller cross section of the single top production along with the very large background from the top pair production meant that the first observation of single top production at Tevatron was made 14 years after the discovery of the top quark [7,8].

There are three separate modes for single top production. They differ according to the associated particle produced with the top and the initial particles producing the top. These processes can be categorized according to the virtuality of the W boson. All these processes involve the Wtb coupling; single top production through the t channel (which has the largest cross section at the LHC), through the s channel and in association with a W boson. The corresponding Feynman diagrams are depicted in Fig. 1.

Single top production, although has smaller rate than $t\bar{t}$ production, is phenomenologically very interesting. First, it allows a direct measurement of V_{tb} in the Cabbibo-Kobayashi-Maskawa mixing matrix [9,10]. Inference on the b-quark density within the proton is possible as well by measuring single top production cross section both through the t-channel and Wt process. In single top quark production, the produced top is highly polarized allowing for a direct test of the $V - A$ structure of weak interaction [11]. Finally, single top production is one of the interesting channels to look for new physics beyond the Standard Model [12–15]. Extensive studies of single top production at hadron colliders including radiative corrections have been performed at NLO [16–24] and NNLO [25–27] in the strong coupling. Furthermore, NLO calculations of single top production matched with parton showers become available within MC@NLO [28,29] and POWHEG [30,31]. Recently, a transverse momentum resummation at NLO + NLL for single top production through the t channel has been

*adil.jueid@sjtu.edu.cn

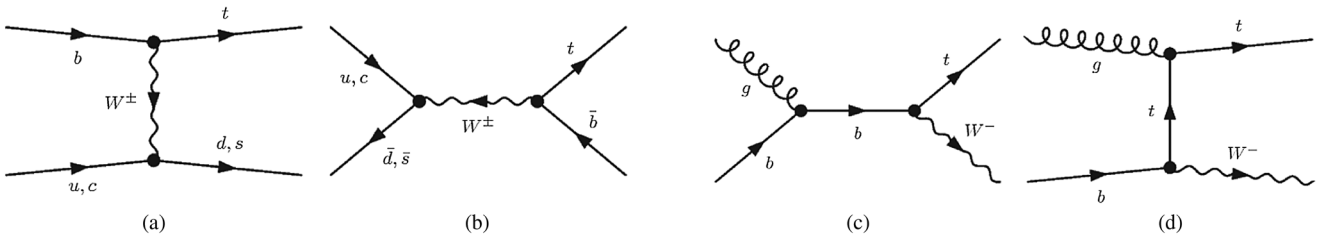

FIG. 1. LO parton level Feynman diagrams of single top production at hadron colliders.

proposed in [32]. Single top production cross sections have been measured by the ATLAS and CMS Collaborations at $\sqrt{s} = 7 \oplus 8$ TeV [33–41] and $\sqrt{s} = 13$ TeV [42–44]. These results were found in agreement with the SM predictions.

The top quark has a very short lifetime, $\tau_t \simeq G_F^{-1} m_t^{-3} \ll m_t/\Lambda_{\rm QCD}^2$, which implies that it decays before hadronization effects take place. Hence, all its properties can be studied by looking at the kinematical distributions of its decay products. The top quark decays with almost a 100% branching fraction into $W^{\pm}b$. Furthermore, due to the weak interaction universality, this process has certain pattern, the so-called $V-A$ structure which manifests itself at the lowest order in perturbation theory. Departures from this universal structure are possible through radiative corrections in the SM and/or new physics effects. This departure might be seen as the presence of the so-called anomalous Wtb couplings. One possible parametrization of these couplings is the use of effective field theoretical approach where $SU(3)_c \otimes SU(2)_L \otimes U(1)_Y$ gauge invariant and 6-dimensional operators are added to the SM Lagrangian [45–48]. A global fit of these operators to the existing data has been recently done in [49–52].

The transition amplitude for top quark decay into a W boson and a b quark can be written as

$$\mathcal{M}(t \to bW^+) = \frac{-e}{\sqrt{2}\sin\theta_W} \bar{u}_b(p_b) \Gamma^{\mu}_{tbW} u_t(p_t) \epsilon^*_{\mu}(q), \quad (1)$$

with

$$\Gamma^{\mu}_{tbW} = -\frac{ig}{\sqrt{2}} \left[\gamma^{\mu}(V_L P_L + V_R P_R) + \frac{i}{M_W} \sigma^{\mu\nu} q_{\nu} (g_L P_L + g_R P_R) \right],$$

where $q = p_t - p_b$ is the momentum of the $W^{\pm}$ boson (which is assumed to be on-shell) and $P_{L,R} = 1/2(1 \pm \gamma_5)$ are the projection operators, V_L, V_R, g_L and g_R are called anomalous couplings. In the SM, at tree level, $V_L = V_{tb}$ and $V_R = g_L = g_R = 0$ whereas EW and QCD radiative corrections induce nonzero values of the anomalous couplings. Computations of the anomalous couplings have been performed in [53–62] both in the SM and certain extensions of it. It was found that SM corrections to anomalous couplings are extremely small, i.e., $g_L = -(1.247 + 0.002747i) \times 10^{-3}$, $g_R = -(8.6 + 2.05i) \times 10^{-3}$ and $V_R = (2.911 + 0.9i) \times 10^{-3}$ [60]. Furthermore, the dominant contribution comes from QCD whereas EW corrections are subleading accounting about 8–15% of the total contribution. Contributions of the anomalous Wtb couplings to various flavor observables have been considered in [63,64].

As mentioned above, the top quark produced in association with a quark or W, is highly polarized. This polarization is decided by the anomalous tbW couplings involved in the production of the single top. The production cross section, the polarization of the top, and the energy distributions of the decay products of the single top all carry information about these anomalous couplings. In fact, recently a study [65] had shown how one can simultaneously study the top polarization as well as the Wtb anomalous coupling and constructed some asymmetries in the observables that are sensitive to both. However, it did not make any reference to a specific top production mechanism. It was pointed out in [66] that measuring accurately single top production cross sections through the t and tW channels would constrain effectively the anomalous Wtb couplings. In this paper, we wish to extend the analysis of the observables suggested in [65] as well as the cross-section information, to the single top production via the t channel.

Thus the aim of this paper is to make a study of the sensitivity of the LHC to the anomalous coupling g_R using energy and angular observables in the t channel single top production at $\sqrt{s} = 13$ TeV. The observables used in our analysis consist of asymmetries based on energy and angular distributions of the top quark decay products. As we will see in this paper, their use will give additional information about the existence of possible anomalous couplings in the Wtb vertex. Since these observables depend on polarization, it is expected that they will be robust against QCD radiative corrections. QCD radiative corrections consist of corrections to the production, to the decay and nonfactorizable corrections. Corrections to the production are not expected to play a role in the predictions that we will show since QCD is a vector theory that is parity conserving, while polarization-based observables are parity-violating. In fact, this was demonstrated explicitly in an analysis of the charged Higgs production [67]. Corrections to the semileptonic

decay of the top quark ($t \to b\nu_\ell \ell$) are very small [68,69]. Nonfactorizable corrections are corrections to the production and subsequent decay; they could be important for some variables near the production-threshold but are exactly zero if the top quark is on-shell.

We use observables suggested in [70], but many of them were proposed long time ago in [65,71] and were used for several studies (see [67,72–75]). In addition, we separate the study into two different categories; parton and particle level. In the former case, no cuts are imposed on the particles' momenta while in the latter loose cuts are imposed. The effects of such kinematical cuts were found to be quite important because these affect the shape of the distributions and hence also the projected limits from the results at the parton level. We stress out that these asymmetries are of extreme importance for future experimental analyses and can be used in several channels that involve the top quark and in different collider machines. We will show, in this paper, that using NLO matrix elements is mandatory for future experimental analyses. In this study, following the limits from $\mathrm{BR}(b \to s\gamma)$, we set $V_R = g_L = 0$ and g_R will be taken to be real.

The paper is outlined as follows: In Sec. II, we review the limits on the anomalous Wtb couplings from direct experimental searches and from statistical fits to several measurements. The setup of the calculation and details about event selection are summarized in Sec. III. In Sec. IV, we show the computations of single top production through the t channel at LO and NLO both in the SM and the SM augmented by anomalous Wtb coupling. The studied observables are briefly discussed in Sec. V. Numerical results and sensitivity projections are shown in Sec. VI. In Sec. VII, we draw our conclusions. Details about the interpolation procedure are shown in the Appendix.

II. LIMITS ON ANOMALOUS Wtb COUPLINGS

Anomalous Wtb couplings are constrained both indirectly from flavor changing decays such as $b \to s + \gamma$ as well as from measurements at both the Tevatron and the LHC: those of helicity fractions of the W produced in top decay, both in pair production of the top as well as the single top production, as well as the spin-spin correlations in top pair production etc. A summary of early constraints can be found in [6]. Measurement of $b \to s + \gamma$ branching ratio constrains V_R, g_L strongly, however g_R is rather weekly constrained [76]. Measurements of the W-boson helicity fraction in top pair production at the Tevatron [77] as well at the LHC [78–80]. In fact, an analysis of a combination of the measurements of the $\mathrm{BR}(b \to s\gamma)$ [76] and the W helicity fractions at the Tevatron [77] together, had shown that $|g_R|$ is the only coupling that could have nontrivial values. The large increase of single top production cross sections with increasing energy, from Tevatron to the LHC, meant that one could also use the single top processes to this end as well [79,81–84]. LHC experiments have used helicity fraction of the W produced in the t decay [78], the double differential decay rate of the singly produced top quark [82], asymmetries constructed out of W-boson angular distributions [84], as well as the triple differential decay distributions for the t quark [85]. In these analyses, limits on various anomalous couplings are obtained under different assumptions; sometimes letting all the couplings vary around their SM values or sometimes keeping some of the couplings fixed at their SM values and so on. Furthermore, depending on the variables used, limits can be obtained on the real or imaginary parts of these anomalous couplings. Analyses that tried to constrain all the anomalous couplings simultaneously, using only the data on single top at

TABLE I. Summary of the limits on anomalous Wtb couplings from $\mathrm{BR}(b \to s\gamma)$ and from direct experimental searches. A complete listing can be found in the PDG [3].

Constraint	Limits	Reference
$\mathrm{BR}(b \to s\gamma)$	$-0.15 < \mathrm{Re}(g_R) < 0.57$, $-7 \times 10^{-4} \le V_R \le 2.5 \times 10^{-3}$ $-1.3 \times 10^{-3} \le g_L \le 4 \times 10^{-4}$	[76]
W helicity fractions	$\mathrm{Re}(V_R) \in [-0.20, 0.23]$, $\mathrm{Re}(g_L) \in [-0.14, 0.11]$, $\mathrm{Re}(g_R) \in [-0.08, 0.04]$.	[78]
	$\mathrm{Re}(g_R) \in [-0.24, 0.20]$, $\mathrm{Re}(g_L) \in [-0.14, 0.10]$	[79]
	$\mathrm{Re}(g_L) \in [-0.30, 0.25]$, $\mathrm{Re}(g_R) \in [-0.15, 0.10]$	[81]
Double differential cross section	$\mathrm{Re}(\frac{g_R}{V_L}) \in [-0.36, 0.10] \mathrm{Im}(\frac{g_R}{V_L}) \in [-0.17, 0.23]$	[82]
t-channel cross section	$V_L > 0.98$, $\lvert V_R \rvert < 0.16$ $\lvert g_L \rvert < 0.057$, $-0.049 < g_R < 0.048$	[83]
W-boson polarization	$V_R \in [-0.24, 0.31]$, $g_L \in [-0.14, 0.11]$, $g_R \in [-0.02, 0.06] \cup [0.74, 0.78]$	[80]
	$\mathrm{Im}(g_R) \in [-0.18, 0.06]$	[84]
Triple differential cross section	$\lvert \frac{V_R}{V_L} \rvert < 0.37$, $\lvert \frac{g_L}{V_L} \rvert < 0.29$ $\mathrm{Re}(\frac{g_R}{V_L}) \in [-0.12, 0.17]$, $\mathrm{Im}(\frac{g_R}{V_L}) \in [-0.07, 0.07]$	[85]

the LHC [83,85] with no assumptions on the value of V_L, still allow values of $|g_R| \sim 0.1$–0.2. Fits assuming $V_L = 1$ from $t\bar{t}$ production [80] by ATLAS also allow large values of $g_R(\sim 0.7)$, but these are in conflict with the cross-section measurements of single top processes and, hence, cannot be taken seriously. On the other hand, a phenomenological analysis of only the collider data, viz. the single top cross sections and W helicity fractions from both the Tevatron and the LHC [86], results in the mildest constraints on $|g_R|$ and V_R.

In addition, a combination of different measurements corresponding to electron and neutron electric dipole moments (EDM), top quark observables, and oblique parameters constrains both the imaginary and real parts of the tensorial couplings g_R and g_L [87,88]. In the end, we note that while the imaginary parts of anomalous tensorial couplings are most severely constrained by EDM's of neutron and electron, $\mathrm{BR}(b \to s\gamma)$ constrains $|g_L|$ and W-helicity fraction from the collider data constrain the $|g_R|$ most effectively. Recentl global fits to the LHC and Tevatron data [89–93] and the limits on g_R are not very strong.

A summary of current limits and analyses can be found in [3]. For reference, we depict some limits from experimental searches and from $\mathrm{BR}(b \to s\gamma)$ in Table I. All this discussion thus tells us that it is of great interest to see how the collider data on the cross section and top polarization in single top production can constrain g_R. We proceed now to discuss the procedure to do so using new observables.

III. SETUP AND EVENT SELECTION

For this study, we consider single top production through the t channel in pp collisions at $\sqrt{s} = 13$ TeV. For electroweak couplings, we use the G_μ-scheme, in which the input parameters are G_F, $\alpha_{\mathrm{em}}(0)$ and M_Z. We choose $G_F = 1.16639 \times 10^{-5}$ GeV^{-2}, $\alpha_{\mathrm{em}}^{-1}(0) = 137$ and $M_Z = 91.188$ GeV. From these input parameters, M_W and $\sin^2\theta_W$ are obtained. Furthermore, the top quark pole mass is chosen to be $m_t = 173.21$ GeV. The computation of single top production cross section was done in the 5FS with massive (massless) b quark at LO (NLO). We use the `NNPDF30` PDF sets [94] with the `LHAPDF6` interpolator tool [95] with $\alpha_s(M_Z) = 0.118$. Throughout this study, we will use fixed factorization and renormalization scales, i.e., $\mu_F = \mu_R = m_t$.

Events are generated with `Madgraph5_aMC@NLO` [96,97] in the SM at leading order (LO) and next-to-leading order (NLO) and the SM with anomalous couplings at LO. The right tensorial anomalous coupling g_R is implemented by hand in a `UFO` model file [98]. The model file was validated by comparing some calculations to several results existing in the literature [66,72] concerning cross-section calculations and several distributions in the t and tW channels and we found excellent agreement. The produced events were decayed with `MadSpin` [99], which uses the method developed in [100] to keep full spin correlations. The decayed events are passed to `PYTHIA8` [101] to include parton showers (ISR and FSR) and hadronization. Parton showering algorithm is based on dipole type $p_\perp$ evolution [102]. The other parameters are set according to the `Monash` tune [103]. We have adopted the `MC@NLO` scheme [104] for consistent matching of hard-scattering matrix elements and parton shower MC. `RIVET` [105] was used for analysis of the events. For jet clustering, we use `FastJet` [106] with an anti-$k_\perp$ algorithm and jet radius $R = 0.4$ [107].

We, first, perform a partonic level analysis (no showers, no soft QCD effects and no cuts on the kinematical quantities). We then, perform a particle level analysis (without detector effects) of the showered events. Throughout this paper, we will show results at both the partonic and the particle levels. For the particle level analysis, we require a topology consisting of exactly one isolated charged lepton (electron or muon), missing energy $E_{\mathrm{T}}^{\mathrm{miss}}$ and at least two jets with at least one of them is b-tagged. First, we require exactly one isolated charged lepton with transverse momentum $p_\perp(\mathrm{lepton}) > 10$ GeV and pseudorapidity $|\eta| < 2.5$. We require at least two jets where one of them is tagged with $|\eta| < 2.5$ and $p_\perp(\mathrm{jet}) \geq 25$ GeV. Further isolation requirements are applied to jets, i.e., the angular separation should be always $\Delta R = \sqrt{\Delta\eta^2 + \Delta\phi^2} > 0.5$ for any two jets in the event and $\Delta R(\mathrm{jet}, \mathrm{lepton}) > 0.4$.

IV. SINGLE TOP PRODUCTION THROUGH THE t CHANNEL

In this section, we discuss single top production cross section in the SM at LO and NLO. We illustrate, at the end of the section, the method that we used to include anomalous Wtb coupling in the production at NLO.

A. LO calculation in the SM

At LO, there are two generic contributions to the t-channel process. The first contribution corresponds to the subprocess,

$$b\,q \to t\,q', \tag{2}$$

and the second contribution represents the subprocess,

$$b\,\bar{q}' \to t\,\bar{q}, \tag{3}$$

where $q = u, c$ and $q' = d, s$. Furthermore, contributions to the t-channel process involving the negligible elements of the Cabbibo-Kobayashi-Maskawa (CKM) mixing matrix such as V_{td} and V_{ts} were not taken into account. We have computed the inclusive LO cross sections at $\sqrt{s} = 13$ TeV. Due to the dominance of the valence u-quark PDF over the sea antiquarks, the subprocess (2) gives the dominant

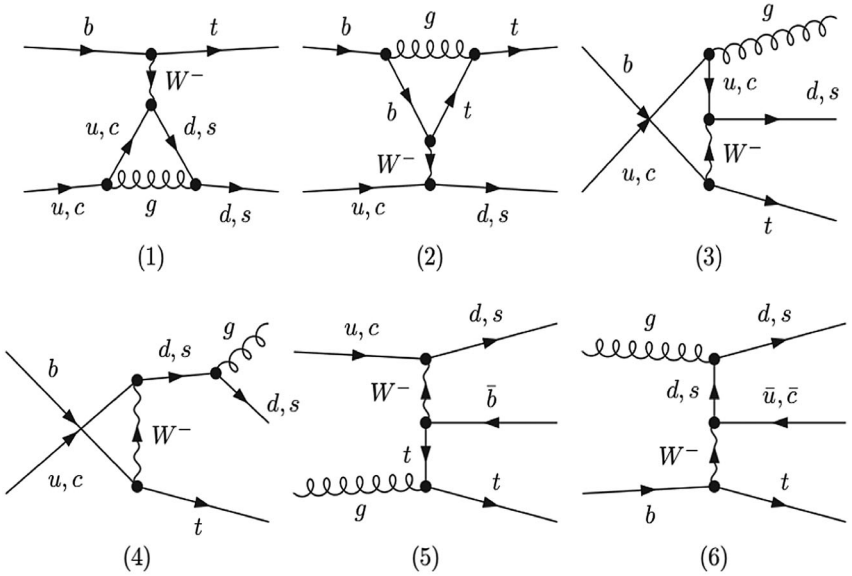

FIG. 2. Feynman diagrams contributing to $bq \to tq'$ subprocess at NLO in the SM where $q = u,\ c$ and $q' = d,\ s$.

contribution which accounts of about 77% of the total cross section.

B. The t-channel at NLO in the SM

Further contributions to the t-channel process, at NLO exist. Such contributions include virtual one-loop corrections to the tree level process as well as tree level $2 \to 3$ real emission processes where the additional emitted parton is soft or collinear. Parton level Feynman diagrams are depicted in Figs. 2 and 3. All the possible flavors that might contribute to this process were included. Due to color conservation, box diagrams do not contribute to the cross section at NLO.

We have computed the total cross section at $\sqrt{s} = 13$ TeV with $\mu_R = \mu_F = m_t$. The dominance of the valence u-quark PDF implies that the cross section from the contribution of Feynman diagrams in Fig. 2 is dominant. We have also estimated theoretical uncertainties on the inclusive cross section both at LO and NLO from scale variations and from PDF. Theoretical uncertainties that are

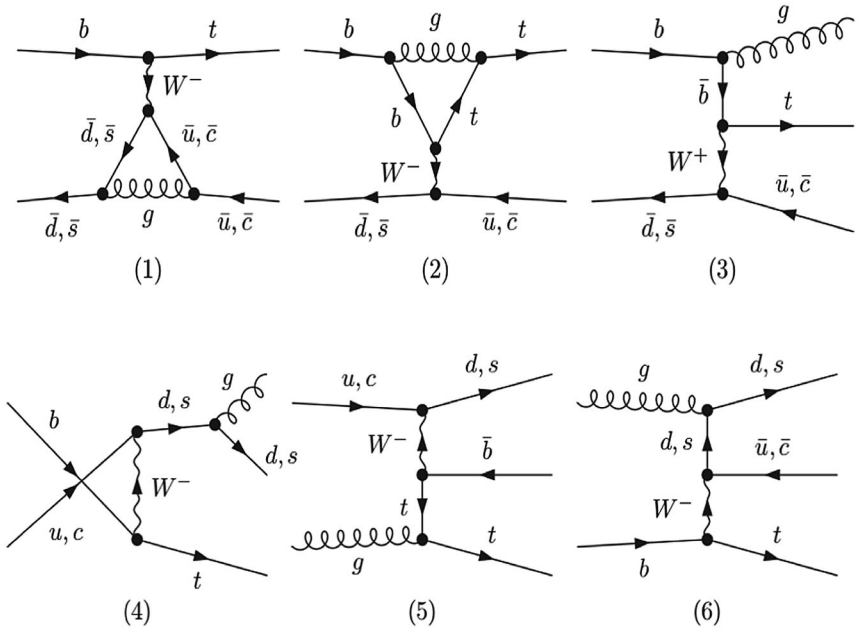

FIG. 3. Feynman diagrams contributing to $b\bar{q}' \to t\bar{q}$ subprocess at NLO in the SM where $q = u,\ c$ and $q' = d,\ s$.

TABLE II. The t-channel production cross section at LO and NLO at $\sqrt{s} = 13$ TeV. Uncertainties due to scale variations and PDF are shown. First rows show the values of the cross section without cuts and in the second rows the cross sections are computed using the cuts highlighted in Sec. III.

Order	σ [pb]	$\delta\sigma_\mu$ [%]	$\delta\sigma_{\rm PDF}$ [%]
LO	128.67	$^{+9.12}_{-11.3}$	± 8.88
	50.50	$^{+10.4}_{-12.5}$	± 9.65
NLO	141.8	$^{+2.8}_{-2.5}$	± 1.2
	75.11	$^{+2.8}_{-2.9}$	± 1.1

due to scale variations are estimated by varying simultaneously the hard factorization and renormalization scales around their nominal values, i.e.,

$$0.5 \leq \mu_R/\mu_{R,0}, \mu_F/\mu_{F,0} \leq 2, \tag{4}$$

where $\mu_{R,0}$ ($\mu_{F,0}$) is the central renormalization (factorization) scale. Thus, obtaining an envelope of the nine possible variations. PDF uncertainties are obtained using the replicas method where each PDF set has one central and 50 members corresponding to the minimal fit and the eigenvectors, respectively. The results for the inclusive cross section at LO and NLO along with their theoretical uncertainties are depicted in Table II. After cuts were imposed, the total rate decreases by a factor of $\simeq$2.5 and $\simeq$1.9 at LO and NLO, respectively. Furthermore, theoretical uncertainties due to scale variations increase in both LO as well as NLO with the former has even larger relative increase than the latter. The most important consequence of imposing cuts on the decay products is that the K-factor of the fiducial cross section increase to about 1.5 while the theoretical uncertainties at LO do not change much. An immediate consequence of such observation is that the fiducial cross section at NLO is outside the allowed range of scale variations' uncertainty at LO since $\sigma_{\rm LO}^{\rm max} = 50.5 + \delta\sigma_\mu^+ \oplus \delta\sigma_{\rm PDF}^+ \approx 58$ pb $< \sigma_{\rm NLO}$. Hence, for any future analysis or fit involving the cross section of the single top through the t channel, at least the calculation at NLO should be used.

C. Including anomalous *Wtb* couplings

The presence of anomalous Wtb couplings modifies single top quark production cross sections. The production cross section of a top quark through the t channel in pp collisions can be expressed as a function of anomalous right tensorial coupling g_R as

$$\sigma_{\text{t-ch}} = \sigma_{\text{t-ch}}^{\rm SM}(1 + \kappa_1 g_R + \kappa_2 |g_R|^2), \tag{5}$$

where $\kappa_{1,2} \equiv \kappa_{1,2}(m_t, m_b, M_W, \sqrt{s})$. They are determined from a fit and are given by

$$\kappa_1 = 0.45485 \quad (0.66433) \qquad \text{without cuts (with cuts)},$$
$$\kappa_2 = 2.05348 \quad (3.21011) \qquad \text{without cuts (with cuts)},$$

at $\sqrt{s} = 13$ TeV. In Eq. (5), $\sigma_{\text{t-ch}}^{\rm SM}$ is the SM cross section at LO (see, e.g., Table II). We can see that imposing cuts strengthens the dependence of the cross section on the anomalous coupling by a factor of $\simeq$1.5. Although the quadratic term is about 5 times larger than the linear one its contribution to the cross section is mild even for the extreme values of g_R, i.e., $g_R = \pm 0.2$. The results we obtained were compared with those presented in [66] and we found excellent agreement.

Taking into account the anomalous Wtb coupling in the production at NLO is not straightforward. The reason is that one cannot renormalize high dimensional operators using the traditional on-shell renormalization schemes. Using alternative schemes for the renormalization of the SM wave functions and parameters will result in large theoretical uncertainties. However, including anomalous Wtb couplings in the production is very interesting since they completely change the chiral structure of the Wtb vertex and, hence, the top quark polarization, which in fact improves the sensitivity of most observables on the anomalous couplings. We include their effects as a shift on the production while neglecting interference between the virtual corrections and tree level amplitudes with anomalous couplings. Hence, three samples will be generated with the first one corresponds to SM amplitude at NLO, the second to the LO amplitude in the SM and the third one to the amplitude with anomalous couplings at tree level. The transition amplitude for the process

$$pp \to t + X \to b\ell^+\nu_\ell + X$$

can be written as

$$\mathcal{M}(\lambda) = \mathcal{P}(\lambda)\mathcal{D}(\lambda), \tag{6}$$

where $\mathcal{P}$ ($\mathcal{D}$) is the production (decay) matrix elements for the top quark.

For convenience (λ) and (λ') stand for the helicity labeling of all particles. The pure SM tree level amplitude (equivalent to $g_R = 0$) is $\mathcal{P}_0^{\rm SM}$. The contribution of the anomalous coupling g_R will only be taken into account at tree level and will be denoted $\mathcal{P}_0^{g_R}$. The full tree-level amplitude, anomalous amplitude, will be denoted $\mathcal{P}_0^{\rm ano.}$, such that

$$\mathcal{P}_0^{\rm ano.} = \mathcal{P}_0^{\rm SM} + \mathcal{P}_0^{g_R} \tag{7}$$

Since the radiative corrections at the level of the decay are very small in the SM (see, e.g., [108]), the decay part will be considered at tree-level only. For the production part, at tree level, with the inclusion of the anomalous part we have

$$\begin{aligned}\mathcal{P}_{\text{tree}}(\lambda,\lambda') &= \mathcal{P}_{\text{LO}}(\lambda,\lambda') \\ &= (\mathcal{P}_0^{\text{SM}}(\lambda)+\mathcal{P}_0^{g_R}(\lambda'))(\mathcal{P}_0^{\text{SM}}(\lambda)+\mathcal{P}_0^{g_R}(\lambda'))^* \\ &\equiv \mathcal{P}_0^{\text{ano.}}(\lambda)\mathcal{P}_0^{\text{ano.}}(\lambda')^*. \end{aligned} \tag{8}$$

The one-loop radiative corrections will only apply to the SM part. The first higher-order contribution consists of the one-loop $2\to 2$ virtual correction that includes also counterterms, $\delta\mathcal{P}_V(\lambda)$. To this one needs to add the pure SM radiative, $2\to 3$ emission. First of all, for the $2\to 2$ one-loop virtual correction and the g_R contribution we may write

$$\begin{aligned}\mathcal{P}_1(\lambda,\lambda') &= (\mathcal{P}_0^{\text{SM}}(\lambda)+\delta\mathcal{P}_V(\lambda)+\mathcal{P}_0^{g_R}(\lambda'))(\mathcal{P}_0^{\text{SM}}(\lambda) \\ &\quad +\delta\mathcal{P}_V(\lambda)+\mathcal{P}_0^{g_R}(\lambda'))^* \\ &\simeq \mathcal{P}_V(\lambda,\lambda')+\mathcal{P}_0^{\text{ano}}(\lambda)\mathcal{P}_0^{\text{ano}}(\lambda')^* \\ &\quad -\mathcal{P}_0^{\text{SM}}(\lambda)\mathcal{P}_0^{\text{SM}}(\lambda')^*, \end{aligned} \tag{9}$$

where

$$\begin{aligned}\mathcal{P}_V(\lambda,\lambda') &= \mathcal{P}_0^{\text{SM}}(\lambda)\mathcal{P}_0^{\text{SM}}(\lambda')^*+\mathcal{P}_0^{\text{SM}}(\lambda)\delta\mathcal{P}_V(\lambda')^* \\ &\quad +\delta\mathcal{P}_V(\lambda)\mathcal{P}_0^{\text{SM}}(\lambda')^* \end{aligned} \tag{10}$$

Including and integrating over real emission, $\mathcal{P}_R^{\text{SM}}(\lambda)$, and adding it to the virtual correction $\mathcal{P}_V(\lambda,\lambda')$ of Eq. (10) will give the full NLO SM result. What we will refer to as the full NLO (including the LO anomalous part) is

$$\begin{aligned}\mathcal{P}_{\text{NLO}}(\lambda,\lambda') &= \underbrace{\mathcal{P}_V(\lambda,\lambda')+\mathcal{P}_R^{\text{SM}}(\lambda,\lambda')}_{\text{sample 1}}+\underbrace{\mathcal{P}_0^{\text{ano.}}(\lambda)\mathcal{P}_0^{\text{ano.}}(\lambda')^*}_{\text{sample 2}} \\ &\quad -\underbrace{\mathcal{P}_0^{\text{SM}}(\lambda)\mathcal{P}_0^{\text{SM}}(\lambda')^*}_{\text{sample 3}}. \end{aligned} \tag{11}$$

In order to reproduce the data including both the NLO SM and the anomalous contribution (with its quadratic part), we generate three samples for the same phase space point—one for the full anomalous part at tree-level, one for the SM tree-level part (which has to be subtracted to avoid double counting), and one for the SM NLO (which includes the SM tree, virtual, and real emission).

V. OBSERVABLES

In this section, we review the observables that we will be using for our analysis of anomalous Wtb couplings. They consist of asymmetries constructed from the energy and angular distributions of the top quark decay products in single top production through the t channel.

We define an asymmetry with respect to a kinematical variable $\mathcal{O}$ by

$$A_{\mathcal{O}} = \frac{\int_{\mathcal{O}_{\text{min}}}^{\mathcal{O}_{\text{R}}}\frac{d\sigma}{d\mathcal{O}}d\mathcal{O}-\int_{\mathcal{O}_{\text{R}}}^{\mathcal{O}_{\text{max}}}\frac{d\sigma}{d\mathcal{O}}d\mathcal{O}}{\int_{\mathcal{O}_{\text{min}}}^{\mathcal{O}_{\text{R}}}\frac{d\sigma}{d\mathcal{O}}d\mathcal{O}+\int_{\mathcal{O}_{\text{R}}}^{\mathcal{O}_{\text{max}}}\frac{d\sigma}{d\mathcal{O}}d\mathcal{O}}, \tag{12}$$

where $\frac{d\sigma}{d\mathcal{O}}=\frac{d\sigma(pp\to tX\to \ell^+\nu_\ell bX)}{d\mathcal{O}}$, $\ell=e,\ \mu$, is the differential cross section of the top quark with respect to the variable $\mathcal{O}$ and $\mathcal{O}_R$ is a reference point around which the asymmetry will be evaluated. $\mathcal{O}_R$ will be chosen such that the evaluated asymmetry is sensitive to the anomalous coupling and allows for a comparison of cases of different values of the parameter. In what follows, kinematical quantities written with a superscript "0" are given in the top quark's rest frame. Otherwise, they are given in the laboratory frame.

A. Lepton polar asymmetry

The polar angle of the charged lepton, denoted by θ_ℓ^0, is defined by

$$\cos\theta_\ell^0 = \frac{\mathbf{p}_\ell\cdot\mathbf{p}_t}{|\mathbf{p}_\ell||\mathbf{p}_t|}, \tag{13}$$

where $\mathbf{p}_\ell$ is the three-momentum of the charged lepton in the top quark rest frame and $\mathbf{p}_t$ is the top quark three-momentum in the laboratory frame. This observable is a good probe of the top quark polarization.[1] However, given that the presence of anomalous coupling changes the chiral structure of the top quark, we expect that it is a good probe of the anomalous coupling too. This can clearly be seen in Fig. 4, where the $\cos\theta_\ell^0$ distribution is plotted in both the SM and for $g_R=\pm 0.1$. We can see that the effect of the anomalous coupling on the $\cos\theta_\ell^0$ is important and can even change the slope of the distribution for $g_R=-0.1$. Although the presence of cuts (right panel of Fig. 4) modifies the sensitivity of this observable, it can be used for searches of the anomalous couplings. However, the measurement of the polar distribution is quite challenging since it requires a full reconstruction of the top quark momentum. This is hard to be achieved due to the presence of missing energy in the semileptonic decay of the top quark. Nevertheless, several measurements of the charged lepton angle in the helicity basis exist, e.g., in the $t\bar{t}$ system [109]. Hence, it can possibly be measured in the t-channel process in the future. From Fig. 4, we define the reference point for the $A_{\theta_\ell^0}$ to be $\cos\theta_\ell^0=0$.

B. Charged lepton energy

In addition to the angular polar distribution in the top quark's rest frame, two other observables constructed from the charged lepton energy are considered here. We define a dimensionless variable, x_ℓ, by

$$x_\ell = \frac{2E_\ell}{m_t}, \tag{14}$$

where E_ℓ is the lepton's energy in a given frame and m_t is the top quark mass. We consider the energy of the charged

[1]The top quark direction of flight in the pp center-of-mass frame defines the spin quantization axis in the helicity basis.

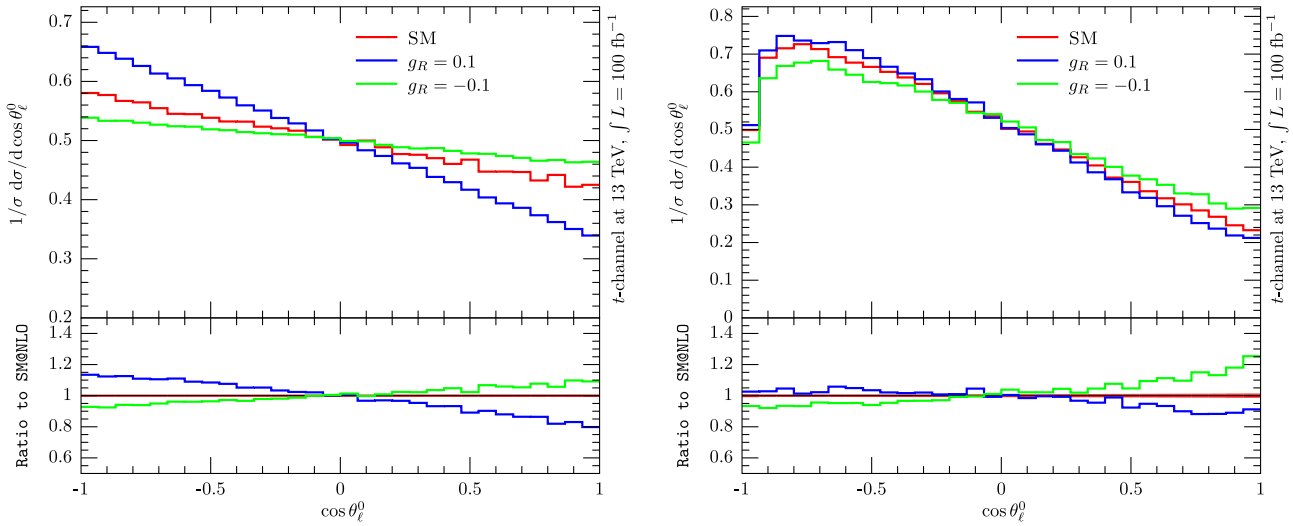

FIG. 4. $\cos\theta_\ell$ distribution in the top quark rest frame using full partonic information (left) and with the cuts implemented at the particle level (right) at NLO.

lepton in two different frames; the top quark's rest frame and the pp center-of-mass frame.

It was shown that, in the top quark's rest frame, this asymmetry is a pure probe of the anomalous Wtb coupling regardless the top quark production mechanism (or in other words top quark polarization) [70]. Hence, at the experimental level, full advantage of this observable should be taken by measuring it in several channels. However, for its measurement, a reconstruction of the top quark momentum is needed. We depict the x_ℓ^0 in the SM and for $g_R = \pm 0.1$ in Fig. 5. The reference point for the corresponding asymmetry, $A_{x_\ell^0}$ is chosen to be $x_{\ell^0,c} = 0.5$, i.e., the value x_ℓ^0 at the peak position in the SM [74].

The situation is different for x_ℓ in the laboratory frame which is shown in Fig. 6. This observable is sensitive to both the anomalous coupling as well as the top polarization. The reason is that under boosts, the energy of the charged lepton becomes

$$E_\ell = \gamma E_{\ell,0}(1 + \beta\cos\theta_\ell^0), \tag{15}$$

where β is the boost factor that takes the charged lepton from the top quark rest frame to the laboratory frame and $\gamma = (1-\beta^2)^{-1/2}$. Given that $\cos\theta_\ell^0$ is directly correlated with top quark polarization, we conclude that x_ℓ is sensitive to the polarization of the top quark as well. The x_ℓ distribution has a high sensitivity to the anomalous

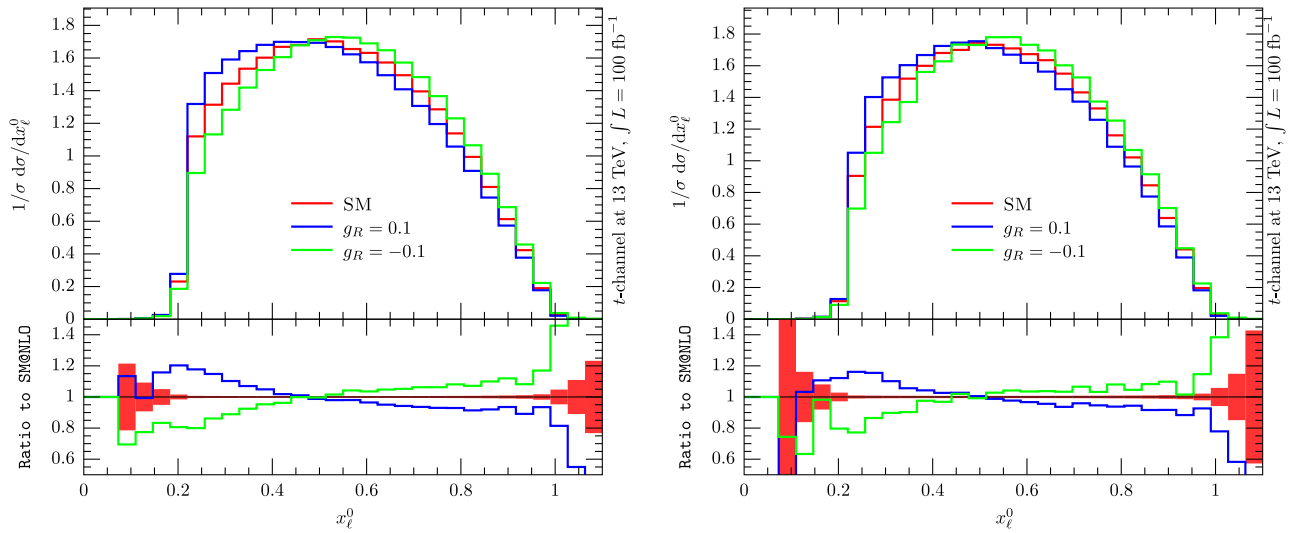

FIG. 5. x_ℓ distribution in the top quark rest frame using full partonic information (left) and with the cuts implemented at the particle level (right) at NLO.

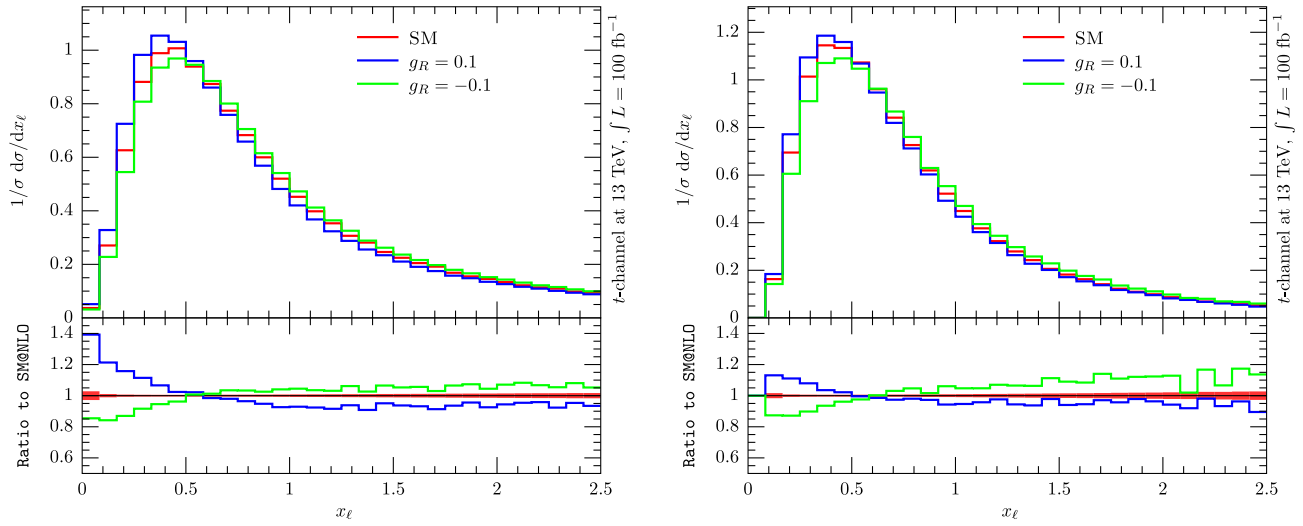

FIG. 6. x_ℓ distribution in the laboratory frame using full partonic information (left) and with the cuts implemented at the particle level (right) at NLO.

coupling for small values of x_ℓ for positive values of g_R and in the full range of x_ℓ for negative values of g_R. However, this observable has a lower sensitivity to the anomalous coupling than x_ℓ^0 due to some cancellations that occur between anomalous couplings and other kinematical factors [70]. Finally, no reconstruction of the top quark momentum is needed in order to measure this observable. A reference point of $x_{\ell,c} = 0.6$ is chosen for the evaluation of the corresponding asymmetry [74].

C. u and z variables

The last two variables from which two different asymmetries will be evaluated have been proposed in [71] as a probe of top quark polarization for highly boosted top quarks. First, a variable u that measures the energy ratio of the charged lepton to the total visible energy (of the top quark decay). This variable is defined by

$$u = \frac{E_\ell}{E_\ell + E_b}, \tag{16}$$

where E_ℓ and E_b are the lepton and b-quark (b-jet) energies in the laboratory frame. It is clear that, from Eq. (16), the u variable is sensitive to both the top polarization and the anomalous Wtb coupling since it can be rewritten as

$$u = \frac{\xi x_{\ell,0}(1+\beta\cos\theta_\ell^0)}{\xi x_{\ell,0}(1+\beta\cos\theta_\ell^0) + (\xi-1)(1+\beta\cos\theta_b^0)}, \tag{17}$$

where $\xi = m_t^2/M_W^2$, $\cos\theta_b^0$ is the polar angle of the b quark in the top quark rest frame and β is the boost factor. From Eq. (17), one can see that the u variable is sensitive to both the anomalous Wtb coupling and top polarization since it involves $x_{\ell,0}$, $\cos\theta_{X,0}$ variables. This is fact is already confirmed by the authors of [70]. We found that including the anomalous Wtb coupling in the production improves the sensitivity of the u variable on g_R. From experimental point of view, it is possible to measure this variable from a simultaneous measurements of the both the charged lepton and b-jet energies in the laboratory frame. This implies that there is no need for reconstructing the top quark momentum. We depict the u variable for three different models at NLO in Fig. 7. From this figure, we choose the reference point $u_c = 0.4$, which is the intersection point of the three different curves corresponding to the SM and to $g_R = \pm 0.1$.

Finally, the z variable, which measures the fraction of the top quark energy taken by the b jet in the laboratory frame, is defined by

$$z = \frac{E_b}{E_t}, \tag{18}$$

where E_b and E_t are the energies of the bottom and top quarks, respectively, in the laboratory frame. Equation (18) can be rewritten to give

$$z = \frac{\xi - 1}{2\xi}(1 + \beta\cos\theta_b^0). \tag{19}$$

Hence, we can see that the z variable has mild sensitivity to the anomalous coupling. Since b quarks are correlated with top quarks, although with a low correlation coefficient $\alpha_b = 40\%$, the z variable is expected to have some sensitivity to the polarization. In Fig. 8, we depict the z variable for the SM and $g_R = \pm 0.1$. We can see that z variable has a lower sensitivity to the anomalous coupling. Furthermore, its measurement requires a determination of the top quark energy, which by itself depends on the decay mode. The hadronic mode, however, has a larger

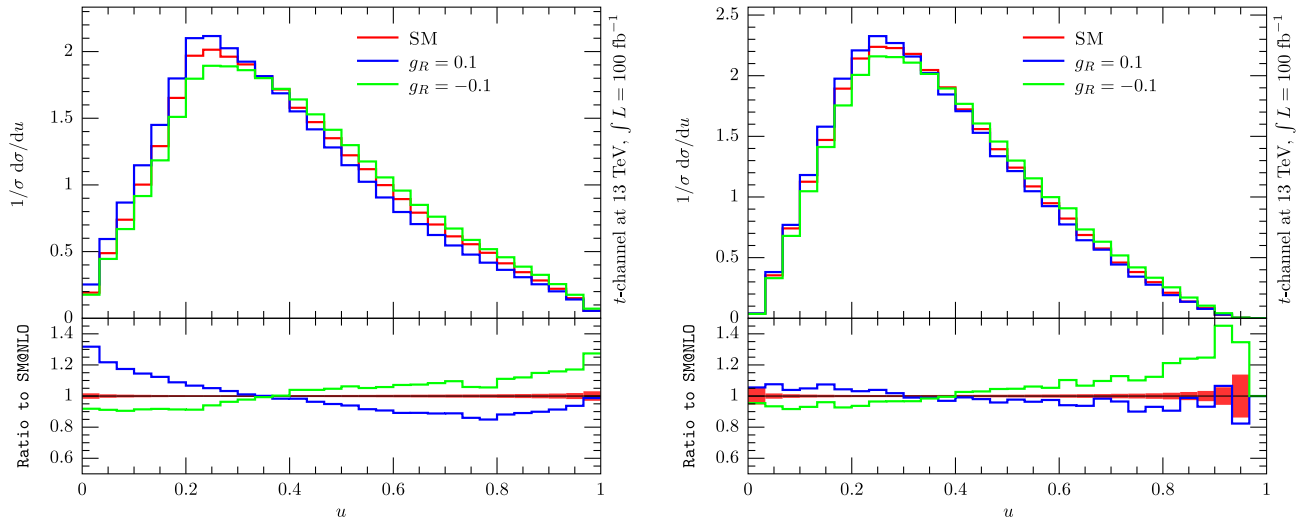

FIG. 7. u distribution in the laboratory frame using full partonic information (left) and with the cuts implemented at the particle level (right) at NLO.

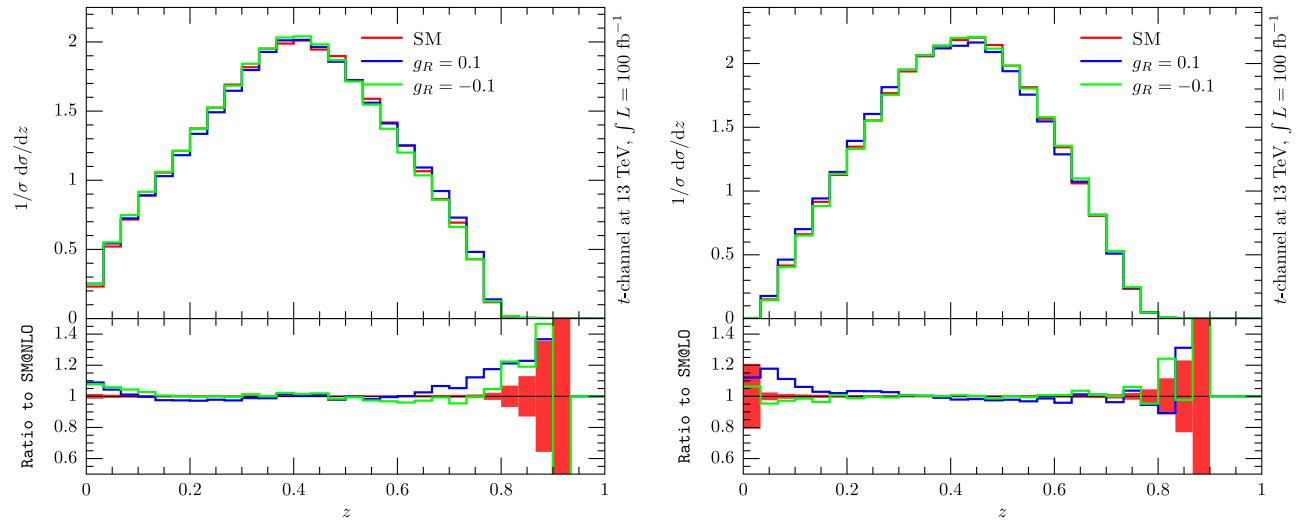

FIG. 8. z distribution in the laboratory frame using full partonic information (left) and with the cuts implemented at the particle level (right) at NLO.

background is better for the measurement of the z variable. The reference point will be chosen to be $z_c = 0.4$.

VI. RESULTS

From the different kinematical distributions shown in Sec. V, asymmetries are constructed (for more details, see the Appendix). These asymmetries present, except A_z, a high sensitivity to the anomalous right tensorial coupling, as it is depicted in Fig. 9, which is weakened at the particle level. We can see that there are some differences between the central values of the asymmetries at LO and NLO of about 6%–30% depending on the particular asymmetry. However, one notices that these differences are within the theoretical uncertainties which are depicted in Table III where only the effect of scale variations is shown. The effect of radiative corrections on the asymmetries depends on the particular variable. At the parton level, two asymmetries are perfectly stable against radiative corrections; i.e., $A_{x_\ell^0}$ and A_u while the others can receive corrections of 6% for $A_{\theta_\ell^0}$, 20% for A_z and 30% for A_{x_ℓ}. On the other hand, the theoretical uncertainties due to scale variations are quite large except for A_u both at LO and NLO and for $A_{x_\ell^0}$ at NLO. At the particle level, the corrections to the asymmetries are lower than to the cross sections with again a strong stability against NLO corrections for $A_{x_\ell^0}$ and A_u. The theoretical uncertainties due to scale variations are lower than in the parton level case with one notable exception, i.e., A_z, which has very large theoretical uncertainties (see Table III).

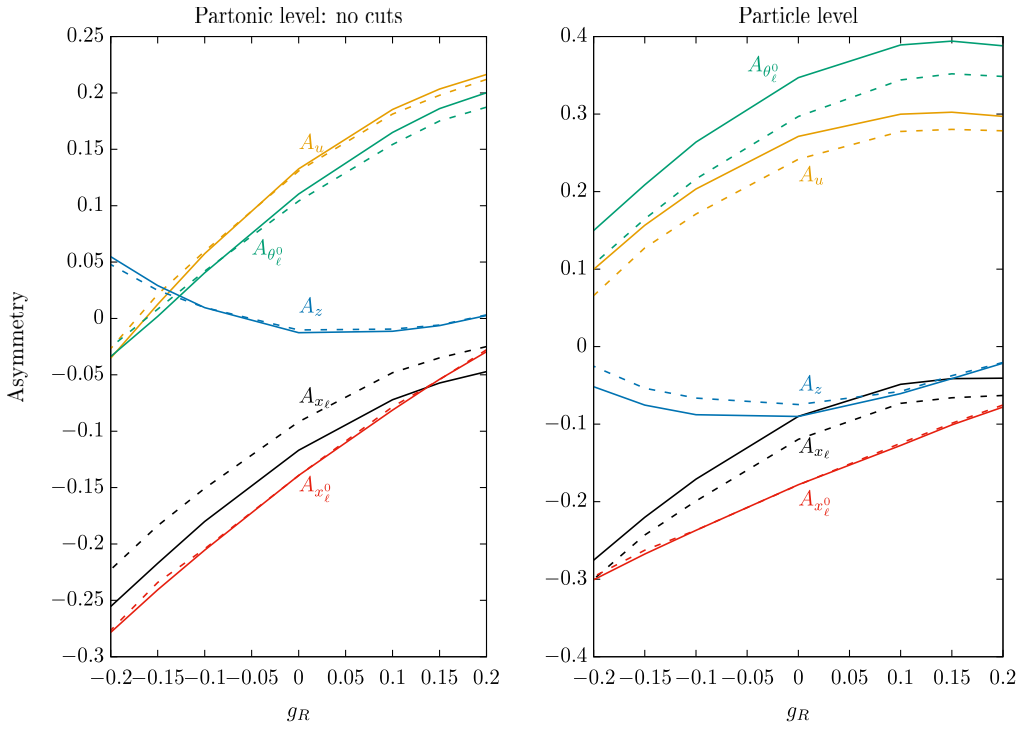

FIG. 9. Dependence of different asymmetries as function of the anomalous coupling at the parton level without cuts (left panel) and at the particle level with cuts (right panel). The solid (dashed) lines show the dependence at LO (NLO).

We perform a χ^2 exclusion to obtain the limits on the anomalous coupling g_R. A χ^2 is defined as follows,

$$\chi^2 = \sum_{\mathcal{O}} \frac{(A_{\mathcal{O}} - A_{\mathcal{O};\mathrm{SM}})^2}{\Delta_{\mathcal{O}}^2}, \tag{20}$$

where $\mathcal{O} = x_\ell$, x_ℓ^0, $\cos\theta_\ell^0$, z and u. $\Delta_{\mathcal{O}}$ is the sum, by quadrature, of the statistical and theoretical uncertainties on the asymmetry $A_{\mathcal{O}}$ in the SM. The former are defined as

$$\Delta_{\mathcal{O}}^{\mathrm{stat.}} = \frac{\sqrt{1 - A_{\mathcal{O}}^2}}{\sqrt{N}}. \tag{21}$$

where N is the number of events

$$N = \sigma_t \mathrm{BR}(t \to b\ell\nu_\ell)\mathcal{L},$$

we assume a luminosity of $\mathcal{L} = 100$ fb^{-1}. Values of g_R are excluded within 1σ, 2σ, and 3σ if the corresponding χ^2 is larger than 2.3,5.99, and 11.8, respectively. We show in Table IV, individual limits obtained from the different

TABLE III. Asymmetries and their theoretical uncertainties in the SM at LO and NLO. The first rows for each asymmetry show the partonic level results while the second rows the particle level ones.

	LO	NLO	NLO/LO
$A_{\theta_\ell^0}$	$0.110^{+0.0000(+0.0\%)}_{-0.01630(-14.5\%)}$	$0.104^{+0.0000(+0.0\%)}_{-0.0155(-14.9\%)}$	0.94
	$0.347^{+0.0000(+0.0\%)}_{-0.0019(-0.5\%)}$	$0.297^{+0.0045(+1.5\%)}_{-0.0023(-0.7\%)}$	0.85
$A_{x_\ell^0}$	$-0.139^{+0.0175(+12.5\%)}_{-0.0000(-0.0\%)}$	$-0.139^{+0.0010(+0.7\%)}_{-0.0000(-0.0\%)}$	1.0
	$-0.178^{+0.0000(+0.0\%)}_{-0.0181(-10.2\%)}$	$-0.178^{+0.0025(+1.4\%)}_{-0.0000(-0.0\%)}$	1.0
A_{x_ℓ}	$-0.117^{+0.0194(+16.5\%)}_{-0.0000(-0.0\%)}$	$-0.091^{+0.0000(+0.0\%)}_{-0.0063(-6.9\%)}$	1.3
	$-0.089^{+0.0000(+0.0\%)}_{-0.0117(-13.1\%)}$	$-0.119^{+0.0073(+6.1\%)}_{-0.0039(-3.2\%)}$	1.3
A_u	$0.133^{+0.0000(+0.0\%)}_{-0.0019(-1.4\%)}$	$0.131^{+0.0000(+0.0\%)}_{-0.0130(-9.9\%)}$	1.0
	$0.271^{+0.0106(+3.9\%)}_{-0.0000(-0.0\%)}$	$0.242^{+0.0019(+0.7\%)}_{-0.0038(-1.5\%)}$	0.9
A_z	$-0.090^{+0.0120(+13.3\%)}_{-0.0000(-0.0\%)}$	$-0.074^{+0.0000(+0.0\%)}_{-0.0024(-3.0\%)}$	0.8
	$-0.013^{+0.0000(+0.0\%)}_{-0.0074(-56.9\%)}$	$-0.010^{+0.0085(+85\%)}_{-0.0000(-0.0\%)}$	0.8

TABLE IV. Individual expected limits at 1σ on the anomalous coupling g_R at LO and NLO using full partonic information (first rows) and at the particle level (second rows).

Asymmetry	LO	NLO
$A_{\theta_\ell^0}$	$[-0.0380, 0.0440]$	$[-0.0480, 0.0541]$
	$[-0.0052, 0.0053]$	$[-0.0082, 0.0086]$
$A_{x_\ell^0}$	$[-0.0417, 0.0446]$	$[-0.0026, 0.0026]$
	$[-0.0486, 0.0542]$	$[-0.0069, 0.0070]$
A_{x_ℓ}	$[-0.0500, 0.0605]$	$[-0.0193, 0.0204]$
	$[-0.0261, 0.0321]$	$[-0.0122, 0.0131]$
A_u	$[-0.0046, 0.0047]$	$[-0.0036, 0.0036]$
	$[-0.0302, 0.0402]$	$[-0.0080, 0.0085]$
A_z	$[-0.0702, 0.1912]$	$[-0.0738, 0.1987]$
	$[-0.1756, 0.0876]$	$[-0.0702, 0.0490]$

TABLE V. Limits on the anomalous coupling g_R at 1σ, 2σ and 3σ at the partonic level without cuts. The first row for each combination represents the interval at LO while the second row represents the NLO exclusion.

Combination	1σ	2σ	3σ
(A_u, A_z, A_{x_ℓ})	$[-0.0046, 0.0047]$	$[-0.0074, 0.0076]$	$[-0.0103, 0.0107]$
	$[-0.0035, 0.0036]$	$[-0.0057, 0.0058]$	$[-0.0079, 0.0082]$
$(A_u, A_{x_\ell}, A_{x_\ell^0})$	$[-0.0046, 0.0046]$	$[-0.0074, 0.0076]$	$[-0.0103, 0.0107]$
	$[-0.0021, 0.0021]$	$[-0.0034, 0.0034]$	$[-0.0047, 0.0048]$
$(A_{x_\ell}, A_{x_\ell^0}, A_{\theta_\ell^0})$	$[-0.0250, 0.0266]$	$[-0.0397, 0.0438]$	$[-0.0547, 0.0629]$
	$[-0.0026, 0.0026]$	$[-0.0042, 0.0042]$	$[-0.0058, 0.0059]$
$(A_u, A_z, A_{\theta_\ell^0})$	$[-0.0046, 0.0046]$	$[-0.0074, 0.0076]$	$[-0.0103, 0.0107]$
	$[-0.0036, 0.0036]$	$[-0.0058, 0.0059]$	$[-0.0080, 0.0083]$
$(A_u, A_z, A_{x_\ell^0})$	$[-0.0046, 0.0046]$	$[-0.0074, 0.0076]$	$[-0.0103, 0.0107]$
	$[-0.0021, 0.0021]$	$[-0.0034, 0.0034]$	$[-0.0048, 0.0048]$
$(A_u, A_{x_\ell}, A_{\theta_\ell^0})$	$[-0.0046, 0.0047]$	$[-0.0074, 0.0076]$	$[-0.0103, 0.0107]$
	$[-0.0035, 0.0036]$	$[-0.0056, 0.0058]$	$[-0.0079, 0.0082]$
$(A_u, A_{x_\ell^0}, A_{\theta_\ell^0})$	$[-0.0046, 0.0046]$	$[-0.0074, 0.0076]$	$[-0.0103, 0.0107]$
	$[-0.0021, 0.0021]$	$[-0.0034, 0.0034]$	$[-0.0047, 0.0048]$
$(A_z, A_{x_\ell}, A_{\theta_\ell^0})$	$[-0.0294, 0.0335]$	$[-0.0458, 0.0562]$	$[-0.0622, 0.0822]$
	$[-0.0178, 0.0189]$	$[-0.0283, 0.0312]$	$[-0.0393, 0.0449]$
$(A_z, A_{x_\ell^0}, A_{\theta_\ell^0})$	$[-0.0274, 0.0299]$	$[-0.0430, 0.0496]$	$[-0.0588, 0.0713]$
	$[-0.0026, 0.0026]$	$[-0.0042, 0.0042]$	$[-0.0059, 0.0059]$
$(A_z, A_{x_\ell}, A_{x_\ell^0})$	$[-0.0309, 0.0348]$	$[-0.0482, 0.0581]$	$[-0.0654, 0.0840]$
	$[-0.0026, 0.0026]$	$[-0.0042, 0.0042]$	$[-0.0059, 0.0059]$

asymmetries at 1σ both at LO and NLO. We can see that all the asymmetries but A_z give strong constraints on the anomalous coupling. Furthermore, the limits placed on the anomalous coupling from A_{x_ℓ} and $A_{\theta_\ell^0}$ are strenghten, at the particle level, by about a factor of 2 and 7, respectively. This is due to the large theoretical uncertainties on those observables at the partonic level which are significantly reduced when showers and cuts are implemented. Overall, constraints on the anomalous right tensorial coupling are stronger at NLO due to the reduction of theoretical and statistical uncertainties. Before discussing the combination of different asymmetries and its effect on the anomalous coupling, we comment about the experimental uncertainties. Generally, measurement of the asymmetries $A_{x_\ell^0}$ and $A_{\theta_\ell^0}$ introduces additional systematic uncertainties since they involve the reconstruction of the top quark rest frame which is very hard for single top production. Hence, although the $A_{x_\ell^0}$ asymmetry is resilient to NLO corrections, it might not be very efficient in the determination of the anomalous coupling. On the other hand, among all the laboratory frame asymmetries, A_u is the most sensitive and involving less systematics (both theoretical and experimental) uncertainties.[2] Combining two asymmetries at one time improves significantly the limits on g_R. We found that combining $A_{x_\ell^0}$ and A_u gives $[-0.0048, 0.0048]$ ($[-0.0021, 0.0021]$) at LO (NLO) at the parton level at 1σ. While at the particle level, those limits are weakened to give $[-0.0261, 0.0312]$ ($[-0.0052, 0.0053]$) at LO (NLO).

These limits can be improved by combining more than one asymmetry at a time. As an example, we estimate projected limits using ten different combinations of the three different asymmetries. We can see in Tables V–VI that the limits are improved by about 1 order of magnitude from those obtained using one asymmetry at a time. In Table V, we show these limits at the partonic level. We can see that, at LO, the six different combinations of the three asymmetries give $g_R \in [-0.0103, 0.0107]$ at 3σ. The situation is different for the NLO case, where the limits are improved by a factor of 2 from the combinations $(A_u, A_{x_\ell}, A_{x_\ell^0})$ and $(A_u, A_{x_\ell^0}, A_{\theta_\ell^0})$ yielding g_R in the interval $[-0.0047, 0.0048]$. On the other hand, including showers and cuts do not change much the limits that we obtain but only the combination of the asymmetries change. In Table VI, we can see that six asymmetries give the strongest limit at LO; i.e., $g_R \in [-0.0112, 0.0121]$. While at NLO, we obtain $g_R \in [-0.0099, 0.0104]$ using the $(A_u, A_{x_\ell^0}, A_{\theta_\ell^0})$ combination. However, as this combination involves the $A_{\theta_\ell^0}$ asymmetry which requires full reconstruction of the top quark direction of motion. Hence, that either the

[2]However, it is expected that experimental systematic errors drop when asymmetries are used.

TABLE VI. Same as Table V but at the particle level.

Combination	1σ	2σ	3σ
(A_u, A_z, A_{x_ℓ})	$[-0.0202, 0.0233]$	$[-0.0314, 0.0403]$	$[-0.0426, 0.0616]$
	$[-0.0067, 0.0070]$	$[-0.0108, 0.0115]$	$[-0.0149, 0.0164]$
$(A_u, A_{x_\ell}, A_{x_\ell^0})$	$[-0.0189, 0.0215]$	$[-0.0294, 0.0368]$	$[-0.0410, 0.0555]$
	$[-0.0048, 0.0049]$	$[-0.0078, 0.0080]$	$[-0.0108, 0.0113]$
$(A_{x_\ell}, A_{x_\ell^0}, A_{\theta_\ell^0})$	$[-0.0050, 0.0052]$	$[-0.0081, 0.0085]$	$[-0.0112, 0.0121]$
	$[-0.0049, 0.0049]$	$[-0.0078, 0.0081]$	$[-0.0110, 0.0114]$
$(A_u, A_z, A_{\theta_\ell^0})$	$[-0.0051, 0.0053]$	$[-0.0081, 0.0086]$	$[-0.0113, 0.0122]$
	$[-0.0058, 0.0059]$	$[-0.0092, 0.0097]$	$[-0.0128, 0.0138]$
$(A_u, A_z, A_{x_\ell^0})$	$[-0.0259, 0.0300]$	$[-0.0461, 0.0515]$	$[-0.0541, 0.0768]$
	$[-0.0053, 0.0054]$	$[-0.0085, 0.0087]$	$[-0.0118, 0.0123]$
$(A_u, A_{x_\ell}, A_{\theta_\ell^0})$	$[-0.0050, 0.0052]$	$[-0.0080, 0.0084]$	$[-0.0114, 0.0120]$
	$[-0.0052, 0.0054]$	$[-0.0084, 0.0088]$	$[-0.0117, 0.0125]$
$(A_u, A_{x_\ell^0}, A_{\theta_\ell^0})$	$[-0.0051, 0.0052]$	$[-0.0081, 0.0085]$	$[-0.0113, 0.0121]$
	$[-0.0044, 0.0045]$	$[-0.0071, 0.0073]$	$[-0.0099, 0.0104]$
$(A_z, A_{x_\ell}, A_{\theta_\ell^0})$	$[-0.0051, 0.0052]$	$[-0.0081, 0.0086]$	$[-0.0112, 0.0121]$
	$[-0.0068, 0.0071]$	$[-0.0109, 0.0116]$	$[-0.0152, 0.0165]$
$(A_z, A_{x_\ell^0}, A_{\theta_\ell^0})$	$[-0.0051, 0.0052]$	$[-0.0082, 0.0086]$	$[-0.0114, 0.0123]$
	$[-0.0053, 0.0054]$	$[-0.0085, 0.0087]$	$[-0.0119, 0.0123]$
$(A_z, A_{x_\ell}, A_{x_\ell^0})$	$[-0.0231, 0.0264]$	$[-0.0363, 0.0447]$	$[-0.0495, 0.0661]$
	$[-0.0060, 0.0061]$	$[-0.0097, 0.0100]$	$[-0.0136, 0.0140]$

(A_u, A_{x_ℓ}, A_z) or $(A_u, A_{x_\ell}, A_{x_\ell^0})$ will do a better job in pinning down the anomalous coupling even the obtained limits are milder than $(A_u, A_{x_\ell^0}, A_{\theta_\ell^0})$.

Now, let us compare our findings with the other results in the literature that used different observables in different channels—W-boson angular observables, single top production cross sections at hadron colliders, etc. In Ref. [110], limits were obtained from single top production at both the Tevatron and the LHC, they obtained $-0.12 < g_R < 0.13$ for the LHC and $-0.24 < g_R < 0.25$ for the Tevatron. In their simulation, they considered pp, $p\bar{p} \to Wb\bar{b}$ and pp, $p\bar{p} \to Wb\bar{b}+$ jet processes at tree level and included V_L, g_L and g_R anomalous couplings using both background contribution as well signal contribution from top quark decays (i.e., s-channel process). In [111], a detailed study of ATLAS sensitivity to the top quark and W-boson polarization in $t\bar{t}$ production using both semileptonic and dileptonic channels was carried out. This analysis was translated to limits on the anomalous Wtb couplings, top quark decay into a charged Higgs boson, and constraints on resonances. Using W boson polarization, and assuming the presence of all the anomalous couplings with $V_L = V_{tb}$, they got limits on g_R, i.e., $g_R \in [-0.065, 0.070]$ at 3σ. Limits on g_R were obtained by the authors of [112] using helicity fractions, some angular and energetic asymmetries and spin-spin correlations observables in $t\bar{t}$ production at the LHC. They obtained $-0.019 < g_R < 0.018$ at the 1σ level by using the A_+ asymmetry defined by

$$A_+ = \frac{N(\cos\theta_\ell^* > z) - N(\cos\theta_\ell^* < z)}{N(\cos\theta_\ell^* > z) + N(\cos\theta_\ell^* < z)} = 3\beta[F_0 + (1+\beta)F_R] \tag{22}$$

where $\cos\theta_\ell^*$ is the polar angle of the charged lepton with respect to the W-boson direction of flight in the W-boson rest frame, $F_{0,R}$ are W-boson helicity fractions, $z = -(2^{2/3}-1)$ is a reference point and $\beta = 2^{1/3}-1$ is a numerical factor. This observable was introduced in order to fully reconstruct the lepton angular distribution in the W-boson rest frame. We notice that the reference value $z = 0$ gives the usual forward-backward asymmetry which is equal to $3/4(F_L - F_R)$. In [112], they assumed the presence of all anomalous Wtb couplings. In [113], sensitivity of the ATLAS experiment on the anomalous Wtb couplings was studied. The study concerned $t\bar{t}$ production with semileptonic final state. In [113], W-boson helicity fractions, ratios of helicity fractions and new angular asymmetries were studied. A systematic study of the different background contributions was carried including detector effects and particle reconstruction effeciencies. All the anomalous couplings were included and individual limits on g_R were obtained by setting $g_L = V_R = 0$ and $V_L = V_{tb}$. The stringent bound on g_R was obtained from the A_- asymmetry, i.e., $g_R \in [-0.0166, 0.0282]$. By setting two couplings to be nonzero at a time and combining four measurements, they got the strongest constraint on g_R, i.e., $[-0.0108, 0.0175]$, which was obtained in combination

with g_L and considerably improves the limit from A_+ alone. In [114], limits on $g_{L,R}$ were obtained using the cross section of single top production through the tW channel at the partonic level assuming $V_L = V_{tb}$ and $V_R = 0$. They obtained $g_R \in [-0.105, 0.041]$ assuming a 25% systematic uncertainties. In Ref. [115], limits on anomalous Wtb couplings were obtained using single top production at the LHC. On the one hand, they obtained limits by combining single top production cross section through the t, s, and tW channels with the ratio R defined by

$$R = \frac{\sigma(pp \to \bar{t} + j)}{\sigma(pp \to t + j)}.$$

They found $g_R \in [-0.10, 0.14]$ assuming $V_R = 0$, $V_L = V_{tb}$ and $g_L \neq 0$. Then, they included top quark decay observables such as W-boson helicity fractions and their ratios. The obtained limit is $-0.012 < g_R < 0.024$ which is about 1 order of magnitude better than those obtained from cross-section measurements alone. In [116], limits on anomalous Wtb couplings were obtained using new proposed observables which consist of angular distributions which probe the W boson polarization and assuming that only one coupling is nonzero at a time or they are either purely real or purely imaginary. They got the following limits at 3σ

$$|\mathrm{Re}(g_R)| > 0.056 \quad \text{from measurement of } A_+,$$
$$|\mathrm{Im}(g_R)| > 0.115 \quad \text{from measurement of } A_{FB}^N,$$

where A_{FB}^N is a proposed asymmetry which vanishes for real anomalous couplings.

The authors of [72], derived limits on the anomalous coupling g_R in tW^- production at the LHC using top quark polarization, charged lepton energy distribution and azimuthal asymmetry at 7 and 14 TeV, they obtained the limit $-0.010 < \mathrm{Re}(g_R) < 0.015$ at 1σ from the combination of three asymmetries assuming $V_L = 1$ and $V_R = g_L = 0$. The authors of [117] obtained limits on the anomalous Wtb couplings from the ATLAS and CMS measurements of single top quark production cross section through the t-channel and top quark decay observables at 7 TeV at 95% CL. Different limits on V_L, V_R, g_L and g_R were obtained by different combinations of the observables. In [118], limits were obtained by considering top quark production at a future Large Hadron electron Collider (LHeC). They proved that the sensitivity to the different anomalous couplings can be significantly improved in this new collider environment using several angular observables. Using tW^- production at the LHC at $\sqrt{s} = 7 \oplus 14$ TeV, the authors of [75] obtained limits on the tensorial right coupling and the anomalous top-gluon coupling by combining the azimuthal asymmetry, top quark polarization and energy asymmetries of the b quark and the charged lepton. They got $g_R \in [-0.03, 0.08]$ at the 1σ level at the parton level.

VII. CONCLUSIONS

In this work, we studied the sensitivity of asymmetries constructed from energy and angular distributions of the top quark's decay products on the anomalous right tensorial coupling in single top production through the t channel at the LHC at $\sqrt{s} = 13$ TeV and with an effective luminosity of 100 fb^{-1}. We included for the first time the contribution of the anomalous coupling in the production with NLO effects. The study was carried both at the parton level and at the particle level with some loose cuts applied on different kinematical variables. We found that asymmetries in the laboratory frame are more suitable to constrain anomalous couplings. However, it is worth to investigate the potential of rest frame observables in the search of anomalous couplings although they need a reconstruction of top quark rest frame. Moreover, these observables present some resilience, within theoretical uncertainties, to next-to-leading order corrections. Furthermore, We found that combination of different asymmetries at one time gives even stronger limits. With their important sensitivity to the anomalous coupling, these observables are competitive with W-boson helicity fractions and other related observables. Hence, taking into account these observables for future experimental searches seems to be indispensable.

ACKNOWLEDGMENTS

The author would like to thank A. Arhrib, F. Boudjema, and R. M. Godbole for their encouragement and their critical comments about the manuscript. The author would like to thank O. Mattelaer, E. Re, P. Skands, and M. Zaro for useful discussions about MC event generation and F. Cornet and S. Nasri for their comments. This work was supported by the Moroccan Ministry of Higher Education and Scientific Research MESRSFC and CNRST: Projet dans les domaines prioritaires de la recherche scientifique et du développement technologique: PPR/2015/6, by Sandwich Educational and Training Program (ICTP), by the GDRI-P2IM Maroc-France (LAPTh), by ENIGMASS, and by Shanghai Pujiang Program. The author would like thank ICTP (Trieste) and LPSC (Grenoble) for providing computational facilities.

APPENDIX: INTERPOLATIONS

From energy and angular based observables, appropriate asymmetries are constructed. We have generated MC samples for each value of the anomalous coupling g_R corresponding to an integrated luminosity of 100 fb^{-1}. The asymmetries were computed for each value of the anomalous coupling

$$g_R \in \{-0.2, -0.15, -0.1, 0.0, 0.1, 0.15, 0.2\}.$$

Where we have investigated the asymmetries both at LO and NLO both at the parton level (without cuts) and at the particle level (with the cuts outlined in Sec. III). To model the behavior of the asymmetries as function of the anomalous coupling, an interpolation to the computed asymmetries was performed. We have adopted a sixth-order polynomial defined as[3]

$$A_{\mathcal{O}} = \sum_{i=0}^{6} \zeta_i^{\mathcal{O}} g_R^i, \tag{A1}$$

where $\zeta_i^{\mathcal{O}}, i = 0, \ldots, 7$ is a set of coefficients determined from the fit and corresponding to the observable $\mathcal{O}$ such that $\zeta_0^{\mathcal{O}} = A_{\mathcal{O}}(\mathrm{SM})$. In Tables VII–VIII, we show the interpolations' results for the different asymmetries.

TABLE VII. The values for the interpolation parameters defined in Eq. (A1) at LO (first rows) and NLO (second rows) using full information at the partonic level.

$A_{\mathcal{O}}$	ζ_0	ζ_1	ζ_2	ζ_3	ζ_4	ζ_5	ζ_6
$A_{\theta_\ell^0}$	0.110	0.620	−0.792	0.526	2.850	−35.518	−0.962
	0.104	0.558	−0.673	0.630	9.076	−32.390	−167.54
$A_{x_\ell^0}$	−0.139	0.618	−0.493	0.299	9.457	−4.994	−159.285
	−0.139	0.680	−0.229	−6.307	4.152	121.203	−161.842
A_{x_ℓ}	−0.117	0.543	−0.919	−0.328	−0.177	−6.157	42.055
	−0.091	0.534	−0.751	−2.562	−1.714	39.264	9.814
A_z	−0.013	−0.09	1.305	−1.500	−15.38	12.78	213.55
	−0.010	−0.089	1.254	−0.591	−26.750	0.989	442.58
A_u	0.133	0.639	−1.143	−0.007	1.615	−6.709	17.189
	0.131	0.638	−1.186	−3.721	17.201	66.602	−284.922

TABLE VIII. The values for the interpolation parameters defined in Eq. (A1) at LO (first rows) and NLO (second rows) using events with kinematical cuts at the particle level.

$A_{\mathcal{O}}$	ζ_0	ζ_1	ζ_2	ζ_3	ζ_4	ζ_5	ζ_6
$A_{\theta_\ell^0}$	0.347	0.628	−2.062	0.0126	−0.026	−20.652	69.380
	0.297	0.651	−1.633	−1.315	−5.174	4.389	63.932
$A_{x_\ell^0}$	−0.178	0.536	−0.608	1.205	23.422	−17.264	−381.304
	−0.178	0.584	−0.451	−2.959	27.175	54.492	−516.980
A_{x_ℓ}	−0.089	0.628	−2.176	−1.906	21.880	21.691	−252.617
	−0.119	0.686	−1.811	−6.792	17.724	111.140	−280.239
A_z	−0.090	−0.150	1.803	−1.320	−25.006	−13.460	334.648
	−0.075	0.0104	1.229	4.397	4.690	−108.563	−75.249
A_u	0.271	0.481	−2.098	0.169	15.691	3.567	−219.977
	0.242	0.574	−1.825	−5.152	11.531	102.039	−234.340

[3]Other functional forms of the interpolation are possible as well and yield similar results.

[1] F. Abe *et al.*, Observation of Top Quark Production in $\bar{p}p$ Collisions, Phys. Rev. Lett. **74**, 2626 (1995).

[2] S. Abachi *et al.*, Observation of the Top Quark, Phys. Rev. Lett. **74**, 2632 (1995).

[3] C. Patrignani *et al.*, Review of particle physics, Chin. Phys. C **40**, 100001 (2016).

[4] M. Beneke *et al.*, Top quark physics, in *1999 CERN Workshop on standard model physics (and more) at the LHC, CERN, Geneva, Switzerland, Proceedings* (2000), p. 419, DOI: 10.5170/CERN-2000-004.

[5] T. Han, The "top priority" at the LHC, Int. J. Mod. Phys. A **23**, 4107 (2008).

[6] W. Bernreuther, Top quark physics at the LHC, J. Phys. G **35**, 083001 (2008).

[7] V. M. Abazov *et al.*, Observation of Single Top Quark Production, Phys. Rev. Lett. **103**, 092001 (2009).

[8] T. Aaltonen *et al.*, First Observation of Electroweak Single Top Quark Production, Phys. Rev. Lett. **103**, 092002 (2009).

[9] J. Alwall, R. Frederix, J. M. Gerard, A. Giammanco, M. Herquet, S. Kalinin, E. Kou, V. Lemaitre, and F. Maltoni, Is V($_{tb}$) ≃1?, Eur. Phys. J. C **49**, 791 (2007).

[10] Q.-H. Cao and B. Yan, Determining V_{tb} at electron-positron colliders, Phys. Rev. D **92**, 094018 (2015).

[11] G. Mahlon and S. J. Parke, Single top quark production at the LHC: Understanding spin, Phys. Lett. B **476**, 323 (2000).

[12] T. M. P. Tait and C. P. Yuan, Single top quark production as a window to physics beyond the standard model, Phys. Rev. D **63**, 014018 (2000).

[13] Q.-H. Cao, J. Wudka, and C. P. Yuan, Search for new physics via single top production at the LHC, Phys. Lett. B **658**, 50 (2007).

[14] Q.-H. Cao, C. S. Li, and C. P. Yuan, Impact of single-top measurement to littlest Higgs model with t-parity, Phys. Lett. B **668**, 24 (2008).

[15] F. Huang, H.-L. Li, S.-Y. Li, Z.-G. Si, W. Su, and Z.-J. Yang, Search for W' signal in single top quark production at the LHC, Chin. Phys. C **42**, 033103 (2018).

[16] J. M. Campbell, R. Frederix, F. Maltoni, and F. Tramontano, Next-to-Leading-Order Predictions for t-Channel Single-Top Production at Hadron Colliders, Phys. Rev. Lett. **102**, 182003 (2009).

[17] G. Bordes and B. van Eijk, Calculating QCD corrections to single top production in hadronic interactions, Nucl. Phys. **B435**, 23 (1995).

[18] T. Stelzer, Z. Sullivan, and S. Willenbrock, Single top quark production via W—gluon fusion at next-to-leading order, Phys. Rev. D **56**, 5919 (1997).

[19] Z. Sullivan, Understanding single-top-quark production and jets at hadron colliders, Phys. Rev. D **70**, 114012 (2004).

[20] J. M. Campbell, R. K. Ellis, and F. Tramontano, Single top production and decay at next-to-leading order, Phys. Rev. D **70**, 094012 (2004).

[21] J. M. Campbell and F. Tramontano, Next-to-leading order corrections to Wt production and decay, Nucl. Phys. **B726**, 109 (2005).

[22] Q.-H. Cao, R. Schwienhorst, and C. P. Yuan, Next-to-leading order corrections to single top quark production and decay at Tevatron. 1. s^- channel process, Phys. Rev. D **71**, 054023 (2005).

[23] Q.-H. Cao, R. Schwienhorst, J. A. Benitez, R. Brock, and C. P. Yuan, Next-to-leading order corrections to single top quark production and decay at the Tevatron: 2. t^- channel process, Phys. Rev. D **72**, 094027 (2005).

[24] E. Bothmann, F. Krauss, and M. Schnherr, Single top-quark production with SHERPA, Eur. Phys. J. C **78**, 220 (2018).

[25] M. Brucherseifer, F. Caola, and K. Melnikov, On the NNLO QCD corrections to single-top production at the LHC, Phys. Lett. B **736**, 58 (2014).

[26] E. L. Berger, J. Gao, C. P. Yuan, and H. X. Zhu, NNLO QCD corrections to t-channel single top-quark production and decay, Phys. Rev. D **94**, 071501 (2016).

[27] E. L. Berger, J. Gao, and H. X. Zhu, Differential distributions for t-channel single top-quark production and decay at next-to-next-to-leading order in QCD, J. High Energy Phys. 11 (2017) 158.

[28] S. Frixione, E. Laenen, P. Motylinski, and B. R. Webber, Single-top production in MC@NLO, J. High Energy Phys. 03 (2006) 092.

[29] S. Frixione, E. Laenen, P. Motylinski, B. R. Webber, and C. D. White, Single-top hadroproduction in association with a W boson, J. High Energy Phys. 07 (2008) 029.

[30] S. Alioli, P. Nason, C. Oleari, and E. Re, NLO single-top production matched with shower in POWHEG: s- and t-channel contributions, J. High Energy Phys. 09 (2009) 111; Erratum, J. High Energy Phys. 02 (2010) 011(E).

[31] E. Re, Single-top Wt-channel production matched with parton showers using the POWHEG method, Eur. Phys. J. C **71**, 1547 (2011).

[32] Q.-H. Cao, P. Sun, B. Yan, C. P. Yuan, and F. Yuan, Transverse momentum resummation for t-channel single top quark production at the LHC (to be published).

[33] G. Aad *et al.*, Comprehensive measurements of t-channel single top-quark production cross sections at $\sqrt{s} = 7$ TeV with the ATLAS detector, Phys. Rev. D **90**, 112006 (2014).

[34] G. Aad *et al.*, Evidence for single top-quark production in the s-channel in proton-proton collisions at $\sqrt{s} = 8$ TeV with the ATLAS detector using the Matrix Element Method, Phys. Lett. B **756**, 228 (2016).

[35] G. Aad *et al.*, Measurement of the production cross-section of a single top quark in association with a W boson at 8 TeV with the ATLAS experiment, J. High Energy Phys. 01 (2016) 064.

[36] V. Khachatryan *et al.*, Measurement of the t-channel single-top-quark production cross section and of the $|V_{tb}|$ CKM matrix element in pp collisions at $\sqrt{s} = 8$ TeV, J. High Energy Phys. 06 (2014) 090.

[37] S. Chatrchyan *et al.*, Measurement of the single-top-quark t-channel cross section in pp collisions at $\sqrt{s} = 7$ TeV, J. High Energy Phys. 12 (2012) 035.

[38] S. Chatrchyan *et al.*, Measurement of the t-Channel Single Top Quark Production Cross Section in pp Collisions at $\sqrt{s} = 7$ TeV, Phys. Rev. Lett. **107**, 091802 (2011).

[39] S. Chatrchyan *et al.*, Observation of the Associated Production of a Single Top Quark and a W Boson in pp Collisions at $\sqrt{s} = 8$ TeV, Phys. Rev. Lett. **112**, 231802 (2014).

[40] S. Chatrchyan *et al.*, Evidence for Associated Production of a Single Top Quark and W Boson in pp Collisions at $\sqrt{s} = 7$ TeV, Phys. Rev. Lett. **110**, 022003 (2013).

[41] V. Khachatryan *et al.*, Search for s channel single top quark production in pp collisions at $\sqrt{s} = 7$ and 8 TeV, J. High Energy Phys. 09 (2016) 027.

[42] M. Aaboud *et al.*, Measurement of the cross-section for producing a W boson in association with a single top quark in pp collisions at $\sqrt{s} = 13$ TeV with ATLAS, J. High Energy Phys. 01 (2018) 063.

[43] M. Aaboud *et al.*, Measurement of the inclusive cross-sections of single top-quark and top-antiquark t-channel production in pp collisions at $\sqrt{s} = 13$ TeV with the ATLAS detector, J. High Energy Phys. 04 (2017) 086.

[44] A. M. Sirunyan *et al.*, Cross section measurement of t-channel single top quark production in pp collisions at sqrt(s) = 13 TeV (to be published).

[45] W. Buchmuller and D. Wyler, Effective lagrangian analysis of new interactions and flavor conservation, Nucl. Phys. **B268**, 621 (1986).

[46] B. Grzadkowski, Z. Hioki, K. Ohkuma, and J. Wudka, Probing anomalous top quark couplings induced by dimension-six operators at photon colliders, Nucl. Phys. **B689**, 108 (2004).

[47] B. Grzadkowski, M. Iskrzynski, M. Misiak, and J. Rosiek, Dimension-six terms in the Standard Model Lagrangian, J. High Energy Phys. 10 (2010) 085.

[48] J. A. Aguilar-Saavedra, A minimal set of top anomalous couplings, Nucl. Phys. **B812**, 181 (2009).

[49] G. Durieux, F. Maltoni, and C. Zhang, Global approach to top-quark flavor-changing interactions, Phys. Rev. D **91**, 074017 (2015).

[50] M. P. Rosello and M. Vos, Constraints on four-fermion interactions from the $t\bar{t}$ charge asymmetry at hadron colliders, Eur. Phys. J. C **76**, 200 (2016).

[51] A. Buckley, C. Englert, J. Ferrando, D. J. Miller, L. Moore, M. Russell, and C. D. White, Constraining top quark effective theory in the LHC Run II era, J. High Energy Phys. 04 (2016) 015.

[52] A. Buckley, C. Englert, J. Ferrando, D. J. Miller, L. Moore, M. Russell, and C. D. White, Global fit of top quark effective theory to data, Phys. Rev. D **92**, 091501 (2015).

[53] A. Czarnecki, QCD corrections to the decay $t \to Wb$ in dimensional regularization, Phys. Lett. B **252**, 467 (1990).

[54] C. S. Li, R. J. Oakes, and T. C. Yuan, QCD corrections to $t \to W^+ b$, Phys. Rev. D **43**, 3759 (1991).

[55] W. Bernreuther, P. Gonzalez, and M. Wiebusch, The top quark decay vertex in Standard Model extensions, Eur. Phys. J. C **60**, 197 (2009).

[56] J. Drobnak, S. Fajfer, and J. F. Kamenik, New physics in $t- > bW$ decay at next-to-leading order in QCD, Phys. Rev. D **82**, 114008 (2010).

[57] G. A. Gonzalez-Sprinberg, R. Martinez, and J. Vidal, Top quark tensor couplings, J. High Energy Phys. 07 (2011) 094; Erratum, J. High Energy Phys. 05 (2013) 117(E).

[58] L. Duarte, G. A. Gonzlez-Sprinberg, and J. Vidal, Top quark anomalous tensor couplings in the two-Higgs-doublet models, J. High Energy Phys. 11 (2013) 114.

[59] G. A. Gonzlez-Sprinberg and J. Vidal, The top quark right coupling in the tbW-vertex, Eur. Phys. J. C **75**, 615 (2015).

[60] A. Arhrib and A. Jueid, tbW anomalous couplings in the two Higgs doublet model, J. High Energy Phys. 08 (2016) 082.

[61] C. Ayala, G. A. Gonzlez-Sprinberg, R. Martinez, and J. Vidal, The top right coupling in the aligned two-Higgs-doublet model, J. High Energy Phys. 03 (2017) 128.

[62] R. Martinez and G. Valencia, Top and bottom tensor couplings from a color octet scalar, Phys. Rev. D **95**, 035041 (2017).

[63] J. Drobnak, S. Fajfer, and J. F. Kamenik, Interplay of $t \to bW$ decay and B_q meson mixing in minimal flavor violating models, Phys. Lett. B **701**, 234 (2011).

[64] J. Drobnak, S. Fajfer, and J. F. Kamenik, Probing anomalous tWb interactions with rare B decays, Nucl. Phys. **B855**, 82 (2012).

[65] R. M. Godbole, S. D. Rindani, and R. K. Singh, Lepton distribution as a probe of new physics in production and decay of the t quark and its polarization, J. High Energy Phys. 12 (2006) 021.

[66] Q.-H. Cao, B. Yan, J.-H. Yu, and C. Zhang, A general analysis of Wtb anomalous couplings, Chin. Phys. C **41**, 063101 (2017).

[67] R. M. Godbole, L. Hartgring, I. Niessen, and C. D. White, Top polarisation studies in $H^- t$ and Wt production, J. High Energy Phys. 01 (2012) 011.

[68] M. Jezabek and J. H. Kuhn, Lepton spectra from heavy quark decay, Nucl. Phys. **B320**, 20 (1989).

[69] A. Czarnecki, M. Jezabek, and J. H. Kuhn, Lepton spectra from decays of polarized top quarks, Nucl. Phys. **B351**, 70 (1991).

[70] V. Arun Prasath, R. M. Godbole, and S. D. Rindani, Longitudinal top polarisation measurement and anomalous Wtb coupling, Eur. Phys. J. C **75**, 402 (2015).

[71] J. Shelton, Polarized tops from new physics: Signals and observables, Phys. Rev. D **79**, 014032 (2009).

[72] S. D. Rindani and P. Sharma, Probing anomalous tbW couplings in single-top production using top polarization at the Large Hadron Collider, J. High Energy Phys. 11 (2011) 082.

[73] G. Belanger, R. M. Godbole, L. Hartgring, and I. Niessen, Top polarization in stop production at the LHC, J. High Energy Phys. 05 (2013) 167.

[74] R. M. Godbole, G. Mendiratta, and S. Rindani, Looking for bSM physics using top-quark polarization and decay-lepton kinematic asymmetries, Phys. Rev. D **92**, 094013 (2015).

[75] S. D. Rindani, P. Sharma, and A. W. Thomas, Polarization of top quark as a probe of its chromomagnetic and chromoelectric couplings in tW production at the Large Hadron Collider, J. High Energy Phys. 10 (2015) 180.

[76] B. Grzadkowski and M. Misiak, Anomalous Wtb coupling effects in the weak radiative B-meson decay, Phys. Rev. D **78**, 077501 (2008); Erratum, Phys. Rev. D **84**, 059903(E) (2011).

[77] V. M. Abazov *et al.*, Combination of searches for anomalous top quark couplings with 5.4 fb^{-1} of $p\bar{p}$ collisions, Phys. Lett. B **713**, 165 (2012).

[78] G. Aad *et al.*, Measurement of the W boson polarization in top quark decays with the ATLAS detector, J. High Energy Phys. 06 (2012) 088.

[79] S. Chatrchyan *et al.*, Measurement of the W-boson helicity in top-quark decays from $t\bar{t}$ production in lepton + jets

events in pp collisions at $\sqrt{s} = 7$ TeV, J. High Energy Phys. 10 (2013) 167.
[80] M. Aaboud *et al.*, Measurement of the W boson polarisation in $t\bar{t}$ events from pp collisions at $\sqrt{s} = 8$ TeV in the lepton + jets channel with ATLAS, Eur. Phys. J. C **77**, 264 (2017).
[81] V. Khachatryan *et al.*, Measurement of the W boson helicity in events with a single reconstructed top quark in pp collisions at $\sqrt{s} = 8$ TeV, J. High Energy Phys. 01 (2015) 053.
[82] G. Aad *et al.*, Search for anomalous couplings in the Wtb vertex from the measurement of double differential angular decay rates of single top quarks produced in the t-channel with the ATLAS detector, J. High Energy Phys. 04 (2016) 023.
[83] V. Khachatryan *et al.*, Search for anomalous Wtb couplings and flavour-changing neutral currents in t-channel single top quark production in pp collisions at $\sqrt{s} = 7$ and 8 TeV, J. High Energy Phys. 02 (2017) 028.
[84] M. Aaboud *et al.*, Probing the W tb vertex structure in t-channel single-top-quark production and decay in pp collisions at $\sqrt{s} = 8$ TeV with the ATLAS detector, J. High Energy Phys. 04 (2017) 124.
[85] M. Aaboud *et al.*, Analysis of the Wtb vertex from the measurement of triple-differential angular decay rates of single top quarks produced in the t-channel at $\sqrt{s} = 8$ TeV with the ATLAS detector (to be published).
[86] M. Fabbrichesi, M. Pinamonti, and A. Tonero, Limits on anomalous top quark gauge couplings from Tevatron and LHC data, Eur. Phys. J. C **74**, 3193 (2014).
[87] V. Cirigliano, W. Dekens, J. de Vries, and E. Mereghetti, Is there room for CP violation in the top-Higgs sector?, Phys. Rev. D **94**, 016002 (2016).
[88] V. Cirigliano, W. Dekens, J. de Vries, and E. Mereghetti, Constraining the top-Higgs sector of the Standard Model effective field theory, Phys. Rev. D **94**, 034031 (2016).
[89] J. L. Birman, F. Dliot, M. C. N. Fiolhais, A. Onofre, and C. M. Pease, New limits on anomalous contributions to the Wtb vertex, Phys. Rev. D **93**, 113021 (2016).
[90] N. Castro, J. Erdmann, C. Grunwald, K. Krninger, and N.-A. Rosien, EFTfitter—A tool for interpreting measurements in the context of effective field theories, Eur. Phys. J. C **76**, 432 (2016).
[91] Z. Hioki, K. Ohkuma, and A. Uejima, Refined analysis and updated constraints on general non-standard tbW couplings, Phys. Lett. B **761**, 219 (2016).
[92] F. Dliot, R. Faria, M. C. N. Fiolhais, P. Lagarelhos, A. Onofre, C. M. Pease, and A. Vasconcelos, Global constraints on top quark anomalous couplings, Phys. Rev. D **97**, 013007 (2018).
[93] Z.-H. Xiong and L. Zhou, Constraints on Wtb anomalous coupling with $B \to X_s\gamma$ and $B_s \to \mu^+\mu^-$ (to be published).
[94] R. D. Ball *et al.*, Parton distributions for the LHC Run II, J. High Energy Phys. 04 (2015) 040.
[95] A. Buckley, J. Ferrando, S. Lloyd, K. Nordstrm, B. Page, M. Rfenacht, M. Schnherr, and G. Watt, LHAPDF6: Parton density access in the LHC precision era, Eur. Phys. J. C **75**, 132 (2015).
[96] J. Alwall, M. Herquet, F. Maltoni, O. Mattelaer, and T. Stelzer, MadGraph 5: Going beyond, J. High Energy Phys. 06 (2011) 128.
[97] J. Alwall, R. Frederix, S. Frixione, V. Hirschi, F. Maltoni, O. Mattelaer, H. S. Shao, T. Stelzer, P. Torrielli, and M. Zaro, The automated computation of tree-level and next-to-leading order differential cross sections, and their matching to parton shower simulations, J. High Energy Phys. 07 (2014) 079.
[98] C. Degrande, C. Duhr, B. Fuks, D. Grellscheid, O. Mattelaer, and T. Reiter, UFO - The Universal FeynRules Output, Comput. Phys. Commun. **183**, 1201 (2012).
[99] P. Artoisenet, R. Frederix, O. Mattelaer, and R. Rietkerk, Automatic spin-entangled decays of heavy resonances in Monte Carlo simulations, J. High Energy Phys. 03 (2013) 015.
[100] S. Frixione, E. Laenen, P. Motylinski, and B. R. Webber, Angular correlations of lepton pairs from vector boson and top quark decays in Monte Carlo simulations, J. High Energy Phys. 04 (2007) 081.
[101] T. Sjöstrand, S. Ask, J. R. Christiansen, R. Corke, N. Desai, P. Ilten, S. Mrenna, S. Prestel, C. O. Rasmussen, and P. Z. Skands, An Introduction to PYTHIA 8.2, Comput. Phys. Commun. **191**, 159 (2015).
[102] T. Sjöstrand and P. Z. Skands, Transverse-momentum-ordered showers and interleaved multiple interactions, Eur. Phys. J. C **39**, 129 (2005).
[103] P. Skands, S. Carrazza, and J. Rojo, Tuning PYTHIA 8.1: The Monash 2013 Tune, Eur. Phys. J. C **74**, 3024 (2014).
[104] S. Frixione and B. R. Webber, Matching NLO QCD computations and parton shower simulations, J. High Energy Phys. 06 (2002) 029.
[105] A. Buckley, J. Butterworth, L. Lonnblad, D. Grellscheid, H. Hoeth, J. Monk, H. Schulz, and F. Siegert, Rivet user manual, Comput. Phys. Commun. **184**, 2803 (2013).
[106] M. Cacciari, G. P. Salam, and G. Soyez, FastJet user manual, Eur. Phys. J. C **72**, 1896 (2012).
[107] M. Cacciari, G. P. Salam, and G. Soyez, The Anti-k(t) jet clustering algorithm, J. High Energy Phys. 04 (2008) 063.
[108] J. Gao, C. S. Li, and H. X. Zhu, Top Quark Decay at Next-to-Next-to Leading Order in QCD, Phys. Rev. Lett. **110**, 042001 (2013).
[109] M. Aaboud *et al.*, Measurements of top quark spin observables in $t\bar{t}$ events using dilepton final states in $\sqrt{s} =$ 8 TeV pp collisions with the ATLAS detector, J. High Energy Phys. 03 (2017) 113.
[110] E. Boos, L. Dudko, and T. Ohl, Complete calculations of $Wb\bar{b}$ and $Wb\bar{b}$ + jet production at Tevatron and LHC: Probing anomalous Wtb couplings in single top production, Eur. Phys. J. C **11**, 473 (1999).
[111] F. Hubaut, E. Monnier, P. Pralavorio, K. Smolek, and V. Simak, ATLAS sensitivity to top quark and W boson polarization in $t\bar{t}$ events, Eur. Phys. J. C **44**, 13 (2005).
[112] J. A. Aguilar-Saavedra, J. Carvalho, N. F. Castro, F. Veloso, and A. Onofre, Probing anomalous Wtb couplings in top pair decays, Eur. Phys. J. C **50**, 519 (2007).
[113] J. A. Aguilar-Saavedra, J. Carvalho, N. F. Castro, A. Onofre, and F. Veloso, ATLAS sensitivity to Wtb anomalous couplings in top quark decays, Eur. Phys. J. C **53**, 689 (2008).
[114] M. Mohammadi Najafabadi, Probing of Wtb anomalous couplings via the tW channel of single top production, J. High Energy Phys. 03 (2008) 024.

[115] J. A. Aguilar-Saavedra, Single top quark production at LHC with anomalous Wtb couplings, Nucl. Phys. **B804**, 160 (2008).

[116] J. A. Aguilar-Saavedra and J. Bernabeu, W polarisation beyond helicity fractions in top quark decays, Nucl. Phys. **B840**, 349 (2010).

[117] J. A. Aguilar-Saavedra, N. F. Castro, and A. Onofre, Constraints on the Wtb vertex from early LHC data, Phys. Rev. D **83**, 117301 (2011).

[118] S. Dutta, A. Goyal, M. Kumar, and B. Mellado, Measuring anomalous Wtb couplings at $e^- p$ collider, Eur. Phys. J. C **75**, 577 (2015).